



HAL
open science

The Impact of Gulf Stream Frontal Eddies on Ecology and Biogeochemistry near Cape Hatteras

Patrick Clifton Gray, Jessica Gronniger, Ivan Sayvelev, Julian Dale, Alexandria K Niebergall, Nicolas Cassar, Anna E Windle, Dana E Hunt, Zackary Johnson, Marina Lévy, et al.

► **To cite this version:**

Patrick Clifton Gray, Jessica Gronniger, Ivan Sayvelev, Julian Dale, Alexandria K Niebergall, et al.. The Impact of Gulf Stream Frontal Eddies on Ecology and Biogeochemistry near Cape Hatteras. 2023. hal-04009187

HAL Id: hal-04009187

<https://cnrs.hal.science/hal-04009187v1>

Preprint submitted on 7 Mar 2023

HAL is a multi-disciplinary open access archive for the deposit and dissemination of scientific research documents, whether they are published or not. The documents may come from teaching and research institutions in France or abroad, or from public or private research centers.

L'archive ouverte pluridisciplinaire **HAL**, est destinée au dépôt et à la diffusion de documents scientifiques de niveau recherche, publiés ou non, émanant des établissements d'enseignement et de recherche français ou étrangers, des laboratoires publics ou privés.

1 **The Impact of Gulf Stream Frontal Eddies on Ecology and Biogeochemistry near**
2 **Cape Hatteras**

3 **Patrick Clifton Gray^{1,2}, Jessica Gronniger¹, Ivan Sayvelev³, Julian Dale¹, Alexandria K.**
4 **Niebergall⁴, Nicolas Cassar⁴, Anna E. Windle⁵, Dana E. Hunt¹, Zackary Johnson¹, Marina**
5 **Lévy⁶, Chris Taylor⁷, Guillaume Bourdin², Ashley Blawas¹, Amanda Lohmann¹, Greg**
6 **Silsbe⁵, David W. Johnston¹**

7 ¹ Duke University Marine Laboratory, Nicholas School of the Environment, Duke University,
8 Beaufort NC, USA

9 ² School of Marine Sciences, University of Maine, Orono, ME, USA

10 ³ U.S. Naval Research Laboratory, Washington, District of Columbia, USA

11 ⁴ Nicholas School of the Environment, Duke University, Durham NC, USA

12 ⁵ Horn Point Laboratory, University of Maryland Center for Environmental Science, Cambridge,
13 MD, USA

14 ⁶ Laboratoire d'Océanographie et du Climat (LOCEAN), Institut Pierre, Sorbonne Université
15 (CNRS/IRD/MNHN), Simon Laplace (IPSL), Paris, France

16 ⁷ NOAA National Centers for Coastal Ocean Science, Beaufort, NC, USA

17

18 Corresponding author: Patrick Gray (patrick.gray@maine.edu)

19

20 **Key Points:**

- 21 • In-depth investigation of a frontal eddy in the Gulf Stream off Cape Hatteras, North
22 Carolina
- 23 • Continued physical and biogeochemical differences are observed between the eddy and
24 adjacent water masses even as it begins to shear apart
- 25 • We share a conceptual model of the ecological impact of frontal eddies with a hypothesis
26 that they supply zooplankton to secondary consumers

27

28

29 **Abstract**

30 Ocean physics and biology can interact in myriad and complex ways. Eddies, features found at
31 many scales in the ocean, can drive substantial changes in physical and biogeochemical fields
32 with major implications for marine ecosystems. Mesoscale eddies are challenging to model and
33 difficult to observe synoptically at sea due to their fine-scale variability yet broad extent. In this
34 work we observed a frontal eddy just north of Cape Hatteras via an intensive hydrographic,
35 biogeochemical, and optical sampling campaign. Frontal eddies occur in western boundary
36 currents around the globe and there are major gaps in our understanding of their ecosystem
37 impacts. In the Gulf Stream, frontal eddies have been studied in the South Atlantic Bight, where
38 they are generally assumed to shear apart passing Cape Hatteras. However, we found that the
39 observed frontal eddy had different physical properties and phytoplankton community
40 composition from adjacent water masses, in addition to continued cyclonic rotation. In this work
41 we first synthesize the overall ecological impacts of frontal eddies in a simple conceptual model.
42 This conceptual model led to the hypothesis that frontal eddies could be well timed to supply
43 zooplankton to secondary consumers off Cape Hatteras where there is a notably high
44 concentration and diversity of top predators. Towards testing this hypothesis and our conceptual
45 model we report on the biogeochemical state of this particular eddy connecting physical and
46 biological dynamics, analyze how it differs from Gulf Stream and shelf waters even in “death”,
47 and refine our initial model with this new data.

48 **Plain Language Summary**

49 Frontal eddies are spinning masses of water (~30km in diameter) that move along western
50 boundary currents like the Gulf Stream. When they form they carry productive coastal water into
51 the Gulf Stream and drive upwelling within their cores. Together this leads to an increase in the
52 amount of phytoplankton within them - much higher compared to surrounding nutrient-limited
53 Gulf Stream water. On the east coast of the United States one common area of frontal eddy
54 formation is just off Charleston, SC. Eddies then travel up the coast and dissipate near Cape
55 Hatteras, NC. In this work we measured a wide range of physical and biological properties of a
56 frontal eddy just north of Cape Hatteras. We compared these properties within the eddy to the
57 coastal water on one side and the Gulf Stream water on the other, finding clear differences in
58 phytoplankton community composition and other physical and chemical properties. Using the
59 results of these observations together with previous studies we share a simple model for how
60 frontal eddies may impact phytoplankton, zooplankton, and fish – hypothesizing that they may
61 contribute to the high diversity and density of top predators off Cape Hatteras.

62 **1 Introduction**

63 Circular currents of water, termed eddies, can trap and transport water properties
64 throughout the ocean, containing and moving hydrographic and biogeochemical properties
65 laterally as they are advected by major currents and vertically by raising or lowering density
66 surfaces (McGillicuddy, 2016). Mesoscale eddies, with spatial scales $O(100\text{km})$ and temporal
67 scales $O(\text{months})$, are often considered the “weather of the ocean” and are a discrete example of
68 biophysical interaction where physics can strongly influence ocean ecology (Clayton et al., 2013;
69 Gaube et al., 2014; Lévy, 2008; Mahadevan, 2016; Williams & Follows, 1998).

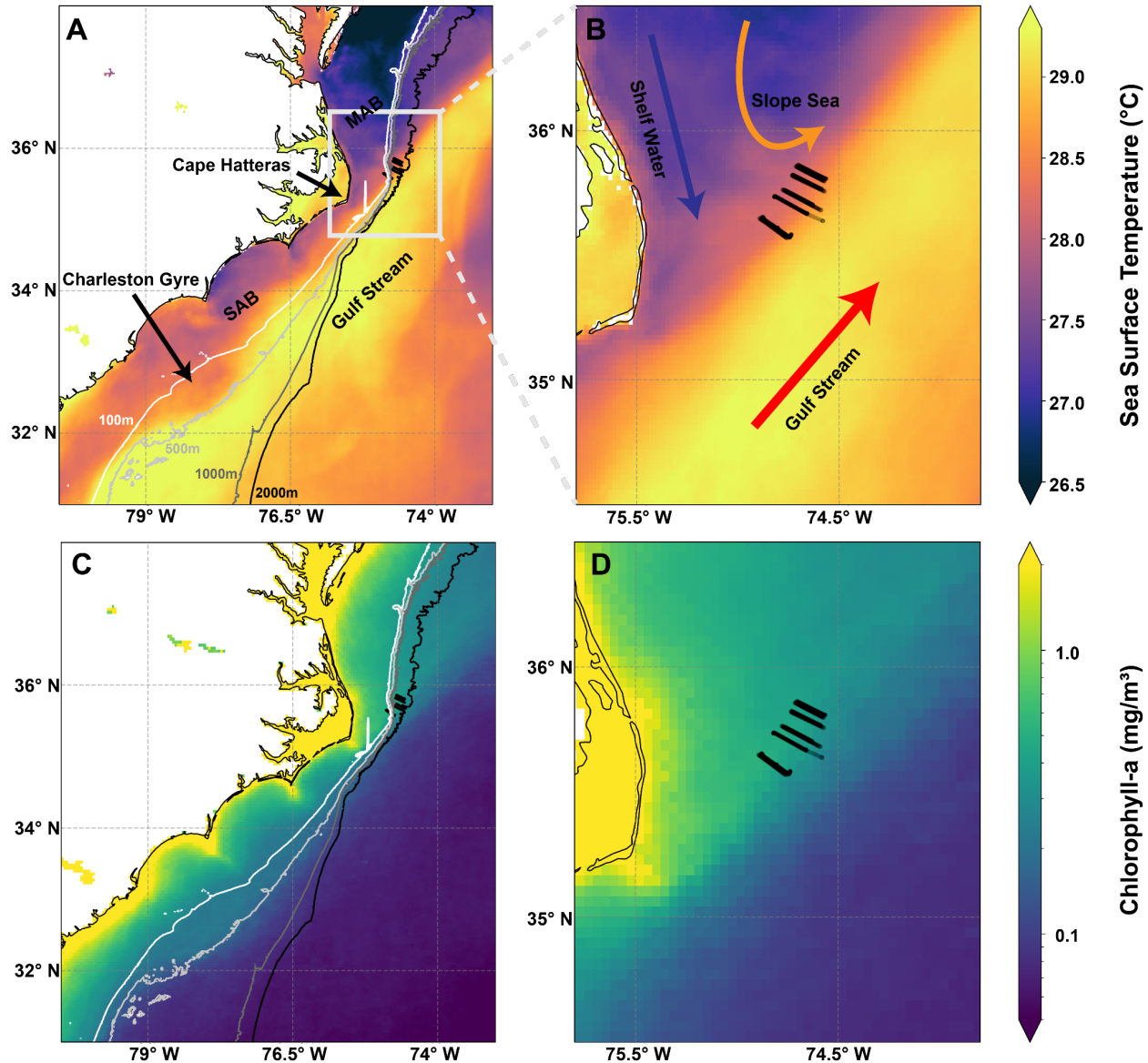
70 The physical processes through which eddies impact ocean ecosystems include trapping
71 and lateral advection, stirring, upwelling and downwelling, and stratification though the

72 ecological impacts of these processes can be complex and contradictory, for a comprehensive
73 review see McGillicuddy (2016). As a specific example, cyclonic eddies from western boundary
74 systems (in the Gulf Stream often called cold core rings) typically have enhanced chlorophyll *a*
75 (chl-*a*) both from entrainment of more nutrient rich and productive coastal water and enhanced
76 upwelling due to isopycnal uplift (Gaube et al., 2014), but with strong winds this could be
77 balanced or even trend negative by wind/eddy Ekman pumping.

78 Given the range of physical and nutrient changes due to eddies, we expect an even more
79 heterogeneous impact on primary productivity, phytoplankton community composition, and even
80 higher trophic levels. Generally where the ecosystem is nutrient limited, cyclonic eddies are
81 associated with increases in phytoplankton size, diversity, and productivity, which lead to
82 increases in zooplankton populations (Belkin et al., 2022; Landry et al., 2008). For long-lived
83 eddies (>6 months), modeling work suggests reduced phytoplankton diversity on average due to
84 competitive exclusion, though individual eddies were widely variable (Lévy et al., 2015). Little
85 work has been done on secondary consumer responses to eddies, though it is likely that after an
86 eddy-induced bloom, transfer efficiency increases as the number of trophic links between the
87 primary consumers and forage fish decreases, e.g. larger phytoplankton such as diatoms
88 consumed by large zooplankton who are consumed directly by fish (Eddy et al., 2021). Eddy-
89 driven productivity and biophysical changes can move up the trophic ladder, structuring the
90 distribution of top predators both due to physiological preferences - anticyclonic eddies deepen
91 the warmer mixed layer allowing sharks to access deeper prey with less temperature stress
92 (Braun et al., 2019; Gaube et al., 2018) - and increased prey density. Thus, an increase in
93 foraging efficiency may explain preferences for eddies in tuna, swordfish, and seabirds
94 (Arostegui et al., 2022; Haney, 1986; Hsu et al., 2015).

95 One class of eddies that are relatively underexplored are frontal eddies, cyclonic features
96 that form in the trough of meanders in western boundary currents such as the Gulf Stream, the
97 Loop Current in the Gulf of Mexico (Maul et al., 1974; Rudnick et al., 2015), the Kuroshio
98 Current (Kasai et al., 2002), and the East Australian Current (Ribbe et al., 2018). On the U.S.
99 eastern seaboard, these features are important for production on the outer shelf of the South
100 Atlantic Bight (T. N. Lee et al., 1991), but they are typically thought to shear apart when the
101 Gulf Stream narrows and rounds Cape Hatteras, North Carolina shortly before the current
102 separates from the continental shelf (Figure 1). In this work we investigated a frontal eddy
103 northeast and downstream of Cape Hatteras, at the Gulf Stream's separation point from the
104 continental shelf. Our goals in this work were to 1) better understand the evolution of primary
105 producers and primary consumers within frontal eddies and 2) re-examine the overall ecosystem
106 impact of frontal eddies throughout their lifetime.

107 Our in-depth in-situ investigation takes place around “the Point” off Cape Hatteras
108 (Figure 1) using a combination of physical, molecular, chemical, and optical methods to
109 elucidate the effects of a cyclonic eddy on ocean biogeochemistry. Given that the in-situ
110 component takes place over just three days - viewed in this work as effectively a single time step
111 - we use satellite data to complement this in-situ view and investigate the two week-long life of
112 this eddy.



113

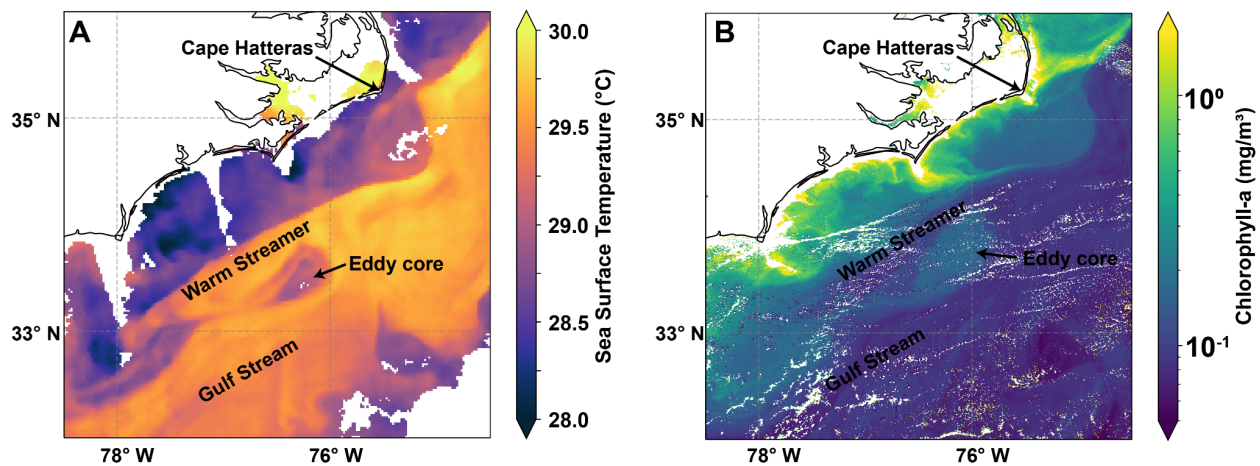
114 **Figure 1.** Study area overview. Panel A shows the broad geographic context using an average
115 sea surface temperature and chlorophyll-a from August 20th to September 10th, the approximate
116 lifetime of our eddy. Bathymetry is shown via the 100m, 500m, 1000m, and 2000m contours.
117 The Gulf Stream is visible as the highest temperature water approximately following the 500m
118 contour until Cape Hatteras. The Charleston Bump is visible in the 500m contour at
119 approximately (34° N, 79° W) and the seaward deflection of the Gulf Stream is visible as a
120 decrease in SST just north of this point. Panel B shows an inset zoom in of our study region with
121 the nine transects shown in black. Panels C and D show the average chlorophyll-a for the same

122 period. SST is from GOES-16 and chl-a is from the Ocean Colour Climate Change Initiative's
123 multi-sensor global satellite chlorophyll-a product.

124 1.1 A Brief History of Frontal Eddy Research

125 There is a long, though intermittent, history of studying frontal eddies in the Gulf Stream
126 (von Arx et al., 1955; Pillsbury, 1890; Webster, 1961). Extensive physical surveys describe these
127 features as cyclonic, cold-core eddies with substantial upwelling through isopycnal uplift (Bane
128 et al., 1981; Thomas N. Lee et al., 1981). In turn, phytoplankton respond intensely to this
129 nutrient upwelling, with observed levels of diatom blooms and chl-a 10-100 times greater than
130 those typically measured in Gulf Stream or outer shelf water (defined as depths from 40-200m
131 (T. N. Lee et al., 1991)). Menhaden and bluefish migrations to the South Atlantic Bight (SAB)
132 are suggested to be secondary to this response of primary producers as the high-levels of
133 phytoplankton provide a consistent food source for higher-level consumers (Yoder et al., 1981).
134 The Frontal Eddy Dynamics experiment in 1987 intensively surveyed a frontal eddy between
135 Cape Lookout and Cape Hatteras, providing some of the first evidence that these features
136 propagate northward and downstream beyond Cape Hatteras, with cross shore and along shore
137 temperature profiles demonstrating the extent of isotherm doming and continued upwelling
138 (Glenn & Ebbesmeyer, 1994b). This work suggested that not only did the feature move past
139 Cape Hatteras, but upwelling continued and a second warm filament formed beyond the cape.
140 The greatest temperature anomalies from upwelling were measured to occur around ~150m
141 depth. Later, a longer survey of frontal eddies in the region confirmed the movement of these
142 eddies north of Cape Hatteras, typically one every 3-7 days, and suggested they are an important
143 and frequent mechanism for transfer from the SAB and Gulf Stream into the Mid Atlantic Bight
144 (MAB) slope sea (Glenn & Ebbesmeyer, 1994a). More recent work has demonstrated that Gulf
145 Stream meanders (including frontal eddies) from the SAB propagate past Cape Hatteras and
146 slowly decay on their way from the Charleston Bump to The Point (Andres, 2021). Yet beyond
147 this work and a few others (Churchill & Cornillon, 1991), the literature often views the North
148 Carolina coast from Cape Lookout northward as a frontal eddy graveyard and thus overlooks the
149 potential for ongoing ecological impacts of these features.

150



151

152 **Figure 2.** Sea surface temperature (Panel A, SST) and chlorophyll *a* (Panel B, chl-*a*) imagery
153 annotated to show the structure of the sampled frontal eddy on August 31st, 2021. The warm
154 streamer is clearly visible as is the cooler and higher chl-*a* eddy core. The chl-*a* image was
155 acquired 13 hours after the SST image so the eddy is slightly further downstream. Another
156 frontal eddy is visible downstream off of Cape Hatteras, though the warm streamer has been
157 pulled into the eddy core and mixed away but is still clearly evident from both the meander in the
158 stream, the beginning of the formation of a new warm streamer, and the positive chl-*a* anomaly.

159 Frontal eddies form where energy is transferred from the mean flow of the current to
160 eddy kinetic energy due to instability processes, often influenced by the local bathymetry. In the
161 northern SAB (Charleston to Cape Lookout, where the eddy in this study formed), this energy
162 transfer is enhanced by the Charleston Bump which deflects the Gulf Stream offshore (Figure 1).
163 When small Gulf Stream meanders with positive vorticity pass through this region, this energy
164 transfer forms mesoscale frontal eddies (see Gula et al 2015 for in depth dynamics). While
165 typically classified as mesoscale eddies, frontal eddies differ from classic Gulf Stream rings as
166 they do not detach from the Gulf Stream, but instead remain trapped within the meander of the
167 current. The main body of the eddy is coastal water entrained by the meander with an upwelled
168 cold core due to the cyclonic rotation. A shallow warm streamer that flows from the downstream
169 meander crest upstream and around this entrained coastal water separates the eddy from other
170 coastal water (Thomas N. Lee et al., 1981). In other regions, specific topographic and current
171 patterns drive energy transfer but the general mechanism and result are similar e.g. East
172 Australian Current (Schaeffer et al., 2017), Kuroshio Current (Kimura et al., 1997).

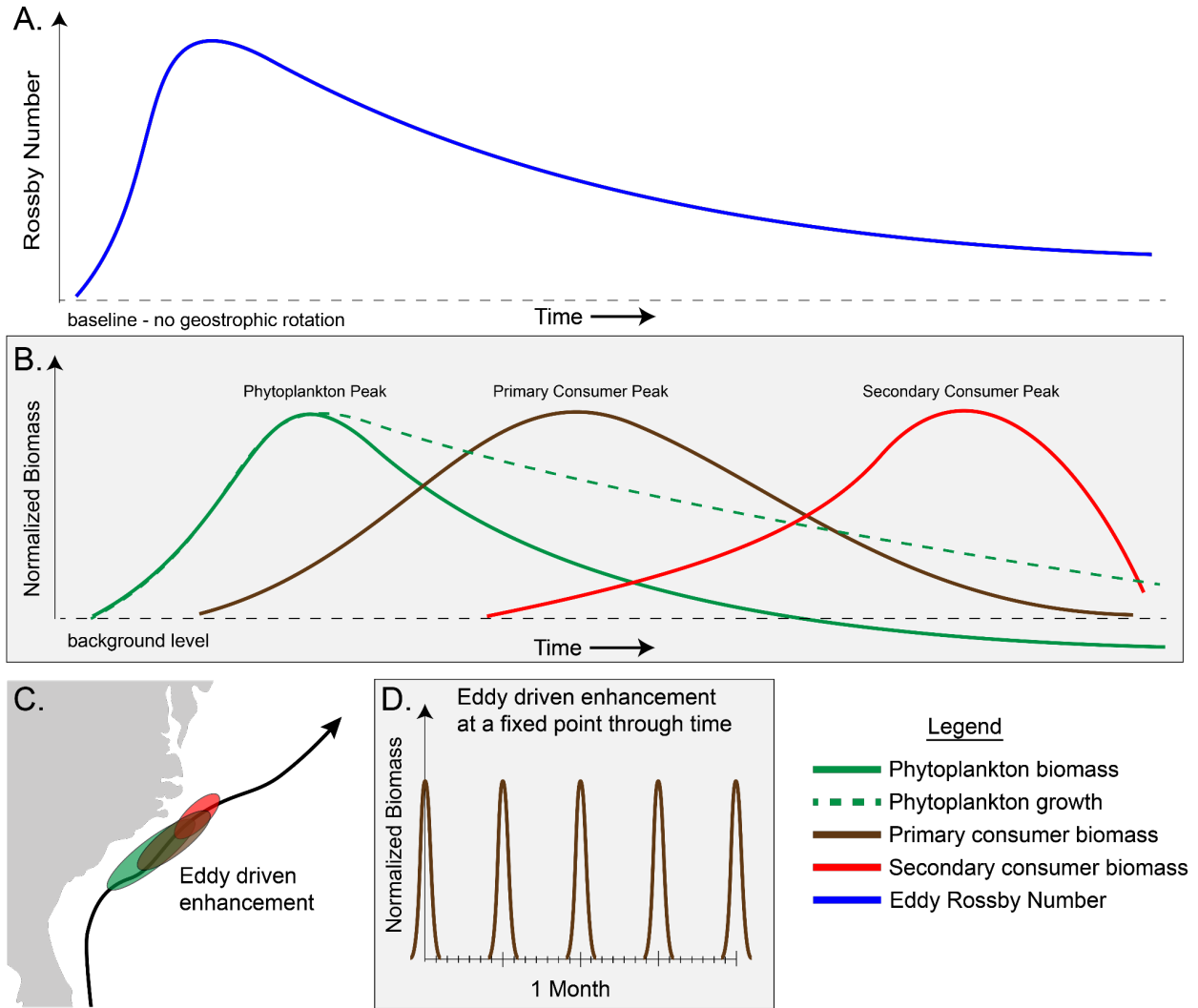
173 Because they are trapped, frontal eddies are subject to shear between Gulf Stream, shelf
174 waters, and dramatic bathymetry gradients. Frontal eddies are also much less nonlinear than
175 typical mesoscale eddies (defined as U/c , the ratio of rotational speed U to the translational speed
176 c of the feature). When $U/c > 1$ the feature is defined as nonlinear, indicating increased
177 coherence. While a typical Gulf Stream ring might be $0.2/0.02$ m/s ~ 10 , a frontal eddy could be
178 approximately $0.5/0.5$ m/s ~ 1 (Glenn and Ebbesmeyer 1994a), suggesting it is less likely to keep
179 a coherent structure as it propagates downstream (Chelton et al., 2011). Differences between
180 frontal eddies and Gulf Stream rings are also described by differences in their Rossby number
181 ($Ro = U/fL$, where U – characteristic velocity, L – characteristic length scale, f – Coriolis
182 frequency), where a smaller Ro indicates a more stable eddy (dominated by geostrophic
183 balance). For our frontal eddy $Ro = 0.5 / (2.5e-5 * 3e4) = 0.66$ compared to a typical Gulf Stream
184 ring at the same latitude where $Ro = 0.2 / (2.5e-5 * 1e5) = 0.008$ suggesting less stability. Rossby
185 numbers for other frontal eddies such as those in the East Australian Current have been reported
186 to be similar or higher (0.6-1.9) (Schaeffer et al., 2017). Compared to other mesoscale eddies,
187 frontal eddies are typically smaller (20-50 km vs. 100+ km), shorter lived (2-3 weeks vs. 6-18
188 months), and form all year at a higher rate (once every 3-7 days). They often occupy nearly half
189 or even a majority of the Gulf Stream-shelf edge in the SAB, thus forming an effective and
190 possibly dominant mechanism for exchange between the Gulf Stream and the shelf (Gula et al.,
191 2015).

192 Depths of frontal eddies are typically 50-200m (Thomas N. Lee, 1975) along stream
193 lengths that are 2-3x cross stream. Frontal eddies in this area typically travel at the same speed as
194 the Gulf Stream meander and are thought to have upwelling on the order of 10 m/day within
195 200m depth. Important to this upwelling is the deep nutrient core of the Gulf Stream, found
196 below 100-200m, with concentrations of nitrate $>10\mu\text{m}$ (Pelegri & Csanady, 1991). Frontal

197 eddies pump the nutrient core up into the euphotic zone via isopycnal uplift driving important
198 nutrient fluxes into the euphotic zone. For eddies formed around the Charleston Bump, this
199 generates considerable productivity from Charleston to Cape Hatteras (T. N. Lee et al., 1991).
200 Recent high resolution modeling ($dx=150m$) shows frontal eddies contain a rich submesoscale
201 field, localized upwelling, and numerous submesoscale eddies forming on the edge of the frontal
202 eddy and the Gulf Stream (Gula et al., 2016) with the possibility for major additional biological
203 implications (Lévy et al., 2018).

204 While the physical and hydrographic dynamics of frontal eddies are reasonably well
205 understood, how these dynamics impact ecosystem function and composition is not well known.
206 Most work concludes that these eddies are sheared apart from the Gulf Stream and left stranded
207 on the outer shelf of the SAB (Lee 1981, 1991), but our work and a few previous studies show
208 that some of these eddies, though they do experience shear from Cape Lookout to Cape Hatteras,
209 are still partially coherent and transport their contents to the MAB and possibly far downstream.
210 In fact, the satellite record shows that a large number of these eddies maintain some coherence
211 past Cape Hatteras and the remnants of frontal eddies and their warm streamers can often be seen
212 in SST imagery as far as the Scotian Shelf (Glenn & Ebbesmeyer, 1994a). Some limited work
213 into the ecosystem implications of frontal eddies in the SAB indicates that the upwelled nutrients
214 are consumed within 2 weeks and this may drive a zooplankton bloom (McClain & Atkinson,
215 1985; Paffenhöfer et al., 1987), though that work assumes nitrate was primarily being fluxed
216 onto the shelf and the eddy was fully dissipating.

217 Based on the literature we developed a simple qualitative conceptual model as a
218 framework for our study (Figure 3). In this model we expect to see a bloom of phytoplankton
219 soon after eddy formation, followed by a zooplankton bloom around a week after the
220 phytoplankton peak, and increased secondary consumers soon after the zooplankton peak. We
221 expect the biology to lag the physics such that phytoplankton growth above the baseline follows
222 upwelling by a day or two and terminates soon after upwelling ends. Our study investigates a
223 single point in time towards the end of the eddy lifetime. Specifically, we examine how physical
224 and biological properties are spatially structured and differ across the Gulf Stream, frontal eddy,
225 MAB slope, and MAB shelf waters and use this along with satellite data, and previous work to
226 understand the natural history of Gulf Stream frontal eddies.



227

228 **Figure 3.** Conceptual model of a frontal eddy from the SAB to the MAB. In Panel A the eddy's
 229 Rossby number is a proxy for geostrophic based upwelling and peaks just after formation and
 230 slowly dissipates as it moves downstream. In Panel B phytoplankton biomass peaks soon (3-5
 231 days) after this peak in upwelling, zooplankton then peaks soon after the phytoplankton peak (5-
 232 7 days), and secondary consumer biomass in the eddy peaks a few days after zooplankton.
 233 Importantly phytoplankton growth is still likely elevated due to upwelling of nutrients even as
 234 standing biomass returns to baseline levels or even below due to grazing. Additionally while
 235 phytoplankton and zooplankton biomass is grown in-place, secondary consumer biomass is not
 236 and instead represents visits. Panel C: while the exact location of these enhancements isn't clear
 237 and is likely variable, this approximately puts the zooplankton enhancement just off Cape
 238 Lookout and Cape Hatteras. Panel D: from a fixed perspective at this peak location, this process
 239 manifests as an enhancement of zooplankton for ~1 day of every 3-7 days year round.

240

1.3 Frontal Eddies and the Gulf Stream's separation point

241

242

243

The in-situ focus area for this study is the confluence of the warm and salty SAB, the relatively fresh and cool MAB slope sea water, the even fresher and cooler MAB shelf waters, and the saltiest and hottest Gulf Stream itself (Seim et al., 2022). The anticyclonic rotation of the

244 subtropical gyre, of which the Gulf Stream is the western expression, converges here with the
245 cyclonic rotation of the slope sea gyre, along with inputs from the MAB shelf water and SAB
246 shelf water (which typically converge at the Hatteras Front). It is a known biodiversity hotspot
247 with some of the highest marine mammal diversity in the world (Byrd et al., 2014), major
248 fisheries for snappers, groupers, tunas, and mackerels, and recreational fishing due to the high
249 density of major sport fish such as tunas and other billfish.

250 We surveyed a frontal eddy just northeast of Cape Hatteras (Figures 1 and 2) in
251 September 2021 with a comprehensive set of tools observing the physical, chemical, and
252 biological status of the region and during both pre-eddy conditions and across the middle of the
253 eddy.

254 The overall objective of this work is to first investigate the biogeochemical status of this
255 frontal eddy past Cape Hatteras, where frontal eddies have rarely been sampled, particularly to
256 see if it contains a different phytoplankton community composition than adjacent waters. Second
257 we assess if the observations suggest an enhancement of grazers that could be supplying
258 secondary consumers in this region. And third we use this new understanding to improve our
259 model of the ecological evolution of eddies from formation to dissolution and their impact on the
260 outer shelf and Gulf Stream ecosystems where they transit.

261 **2 Materials and Methods**

262 **2.1 Focal Region**

263 The eddy studied in this work formed off the Charleston Bump on August 25th-26th,
264 moved past Cape Hatteras on Sept 4th, was surveyed on Sept 5th, 6th, and 7th and moved rapidly
265 downstream and was dissipating, but still apparent by Sept 9th.

266 **2.2 Ship transects**

267 Transects on the R/V Shearwater transited the North Wall of the Gulf Stream in approx
268 10-15 km lines with five data intensive day time transects and four less data intensive night time
269 transects. Transects were planned to cross the front between the shelf and eddy or shelf and Gulf
270 Stream water. In this work we collected nine transects, five in the daytime with a more intensive
271 approach, and four at night (Figures 1, 4 and S1).

272 **2.3 Temperature and Salinity**

273 Temperature and salinity were collected with a SeaBird SBE38 Thermosalinograph
274 collected via the Shearwater's flow through system from an intake at approximately 1.5m depth.
275 This data was logged once per second.

276 **2.4 Chl-a sampling**

277 In-situ chl-a was measured by filtering 100 mL of seawater onto combusted 0.7 μm GF/F
278 filters, extracting in 100% methanol for 48 hours, and reading fluorescence on a chlorophyll
279 calibrated Turner 10AU fluorometer equipped with Welschmeyer filters (Johnson et al., 2010).

280

281 2.5 Flow cytometry

282 Duplicate whole seawater samples were collected from the ship's flow through system at
283 1m depth, fixed with net 0.125% glutaraldehyde and stored at -80 °C until processing.
284 Prokaryotic phytoplankton populations were enumerated using a Becton Dickinson
285 FACSCalibur Flow Cytometer and categorized as previously described (Johnson et al., 2010).
286 Bacterioplankton were quantified using SYBR Green-I on the Attune NxT acoustic flow
287 cytometer (Life Technologies) (Marie et al., 1997).

288 2.6 Nutrients

289 Nutrients were collected by filtering duplicate ~50mL samples through 0.22 μm Sterivex
290 filters which was stored at -80 °C until analysis at the UCSD Nutrient Analysis facility
291 (<https://scripps.ucsd.edu/ships/shipboard-technical-support/odf/chemistry-services/nutrients>)
292 where a Seal Analytical continuous-flow AutoAnalyzer-3 was used to measure silicate, nitrate,
293 nitrite, phosphate, and ammonia using the analytical methods described by (Atlas et al., 1971;
294 Gordon et al., 1992; Hager et al., 1972).

295 2.7 Optical and CDOM

296 Hyperspectral absorption (a), attenuation (c), and the volume scattering function (VSF) at
297 120 deg and 470, 532, and 650 nm were measured continuously (4 Hz, 4 Hz, and 1 Hz
298 respectively) for the duration of this work. a and c were measured at 81 wavelengths 399 to 736
299 nm using a WetLabs ACS spectrophotometer and VSF was measured at 120 deg at 470, 532, and
300 650 nm using a WetLabs ECO-BB3 which was converted to backscattering (b_b) measurements.
301 Both instruments were manually switched between running 0.2 μm filtered sea water and total
302 ("normal") sea water the rest of the time. Filtered seawater was run before and after each transect
303 and absorption, attenuation, and backscattering during the filtered period were linearly
304 interpolated and subtracted from the total sea water values to get the particulate a (a_p), c (c_p), and
305 b_b (b_{bp}). This setup allows retrieval of particulate optical properties independently from
306 instrument drift and biofouling (Slade et al., 2010). This data was collected using Inlinino
307 (Haëntjens & Boss, 2020), an open-source logging and visualization program, processed using
308 InlineAnalysis (<https://github.com/OceanOptics/InLineAnalysis>) following (E. Boss et al., 2019).
309 Colored dissolved organic matter (CDOM) was also measured with a Seapoint Ultraviolet
310 Fluorometer logged on a DataQ DI-2108 to Inlinino. (See supplemental material for more
311 detailed processing overview)

312 These inherent optical properties (i.e., absorption, attenuation, and backscattering) and
313 products calculated from them were used as proxies for a range of particulate properties. γ ,
314 which is estimated as the spectral slope of c_p , is a strong proxy for particle size distribution with
315 a higher γ indicating smaller average particle sizes (Emmanuel Boss et al., 2001). Scattering is
316 driven primarily by particle concentrations, and backscattering is sensitive to both particle
317 refractive index and concentrations, thus the backscattering ratio (i.e. backscattering to
318 scattering) normalizes concentration and varies primarily with refractive index, serving as a
319 proxy for particle composition (Twardowski et al., 2001). A proxy for phytoplankton size
320 (HH_G50) based on anomalous dispersion in the narrow chl- a absorption band around 676 nm is
321 also reported (Houskeeper et al., 2020). The last optical proxy we used is phytoplankton pigment
322 concentrations derived from a gaussian decomposition of the particulate absorption spectrum
323 following (Chase et al., 2013). This approach uses a series of gaussians placed at the same

324 location as various pigment absorption peaks and minimizes the difference between a spectrum
325 constructed of these gaussians with the measured spectrum. This gives the approximate
326 concentration of a range of pigments that can be used as a proxy for various phytoplankton
327 taxonomic groups.

328 2.8 Underway Profiling

329 Profiles were conducted with a Rockland Scientific VMP-250 which collects S, T,
330 chlorophyll-a fluorescence, turbidity (via optical backscatter at 880nm), and turbulence. This
331 instrument was operated in a tow-yo mode on a winch which allowed it to freefall and then be
332 quickly reeled back in and repeated. Profiles were deployed to roughly 100m depth
333 approximately every 500-800m along track. Only downcasts were used.

334 2.9 O₂/Ar-based Net Community Production

335 Net Community Production (NCP), a measure of the net production minus net respiration
336 in the system, was estimated by continuously measuring O₂/Ar ratios in the seawater using
337 Equilibrator Inlet Mass Spectrometry. Briefly, the biological oxygen supersaturation in the
338 mixed layer was calculated following:

$$339 \quad \Delta \left(\frac{O_2}{Ar} \right) = \left[\frac{\left(\frac{O_2}{Ar} \right)_{meas} - 1}{\left(\frac{O_2}{Ar} \right)_{sat}} \right]$$

340 where $(O_2/Ar)_{meas}$ is the ratio of O₂ and Ar measured in the seawater and $(O_2/Ar)_{sat}$ is the ratio of
341 O₂ and Ar in the air. Mixed layer depth (MLD) was calculated using a change of 0.1kg m⁻³ from
342 the surface density based on VMP-250 profiles. MLD was interpolated linearly to get to 2-
343 minute average ML. MLD was fairly consistent in the shelf, slope, eddy, and Gulf Stream water
344 types and thus night time MLD was based on day time MLDs and water type. NCP was
345 calculated following:

$$346 \quad NCP = \Delta \left(\frac{O_2}{Ar} \right) \times O_{2sat} \times \rho \times k$$

347 where O_{2sat} represents the saturated oxygen concentration ($\mu\text{mol kg}^{-1}$) ([Garcia and Gordon 1992](#)),
348 ρ represents the density of the seawater (kg m^{-3}), and k represents the weighted gas transfer
349 velocity (m d^{-1}) calculated following ([Wanninkhof, 2014](#)) and ([Reuer et al., 2007](#)), with
350 modifications from ([Teeter et al., 2018](#)). NCP is reported here in units of $\text{mmol O}_2 \text{ m}^{-2} \text{ d}^{-1}$. 6-
351 hour wind speed data were downloaded from the ERA 5 REanalysis dataset
352 (<https://www.ecmwf.int/en/forecasts/datasets/reanalysis-datasets/era5>). More detailed NCP
353 calculation methods can be found in ([Cassar et al., 2009](#)).

354 2.10 ADCP

355 Ocean velocity data was collected using a Nortek Signature 500 VM Acoustic Doppler
356 Current Profiler. This instrument operates at 500kHz and collects horizontal current vectors and
357 acoustic backscatter. From this, current speed, direction, and shear were calculated along with
358 backscatter strength. Vertical profiles of these measurements were binned in 1m increments from
359 ~1 to 60m depth.

360

361 2.11 Satellite data

362 We used multiple ocean-observing satellites to provide context for the vessel-based
363 sampling. Chl-a products were derived from the European Commission Copernicus programmes
364 Sentinel-3's Ocean and Land Color Instrument (OLCI) and the Ocean Colour Climate Change
365 Initiative's multi-sensor global satellite chl-a product (Sathyendranath et al., 2019). The OLCI
366 data was used to track chl-a within the eddy over its lifetime. Sea surface temperature products
367 were from the Geostationary Operational Environmental Satellite 16 (GOES-16). OLCI Level 2
368 and obtained from <https://codas.eumetsat.int>, OC-CCI chl-a was version 5.0 eight day composites
369 from <https://www.oceancolour.org/>, and GOES-16 hourly SST was acquired from
370 <https://cwcmom.aoml.noaa.gov/erddap/griddap/goes16SSThourly.html>.

371 2.12 Delineating the water masses based on Salinity and Temperature

372 Analysis is primarily based on a continuous view of water properties, given the amount
373 of turbulent mixing occurring along the front, but we also divide water masses into discrete
374 categories of shelf, slope, eddy, and Gulf Stream based on temperature and salinity. That
375 delineation is done by categorizing all water where Shelf < 34 PSU, 35.75 PSU > Slope > 34
376 PSU, 28.2 C > Eddy > 35.75 PSU, and Gulf Stream > 28.2 °C as shown by the T-S diagram in
377 Figure 4 and 5.

378 2.13 Eddy Microbiome

379 A companion study was conducted which focused on the microbiome of the eddy and
380 adjacent water masses (Gronniger et al., 2023). This companion work ran 16SrRNA gene
381 sequencing on the same water samples as our flow cytometry and nutrient analysis and compares
382 the genetic makeup of microbes across the physical structures we studied. The results of
383 Gronniger et al (2023)'s work are summarized and included in the discussion of this study for
384 context.

385 3 Results

386 Our data indicate multiple distinct water masses and clear transitions between the shelf,
387 slope, eddy, and Gulf Stream water (Figure S2). While most biogeochemical properties shift
388 gradually and monotonically across water types, some measured parameters cluster into four
389 distinct groups matching the independent discrete T-S based definitions (Figure 5). Salinity and
390 temperature increase from shelf to slope to eddy to Gulf Stream, while CDOM, phytoplankton
391 size, *Synechococcus*, and bacteria all decrease along this continuum. Physically, the eddy water
392 is similar to Gulf Stream salinity, but is slightly cooler in temperature and thus denser. After
393 classifying water masses based on T and S more nuanced patterns are visible (Figure 6). At first
394 glance, the eddy appears to be on the continuum between slope and Gulf Stream water or, at
395 times, indistinguishable from the Gulf Stream. This is true for most of the optical proxies.
396 Measurements of c_p are similar in the shelf, slope, eddy, and Gulf Stream waters (Figure S4). c_p
397 is dominated by b_p in all water masses, though a_p is a substantially larger proportion of c_p in the
398 400-500nm range in the shelf compared to eddy and Gulf Stream water (Figure S5) as we might
399 expect given the higher chl-a concentrations on the shelf. The backscattering ratio at 440nm
400 (representative of refractive index and thus composition) generally decreases marginally as we
401 move offshore, indicating slightly more organic relative to inorganic particles. Phytoplankton
402 size (via HH_G50) decreases monotonically with CDOM as we move offshore, though

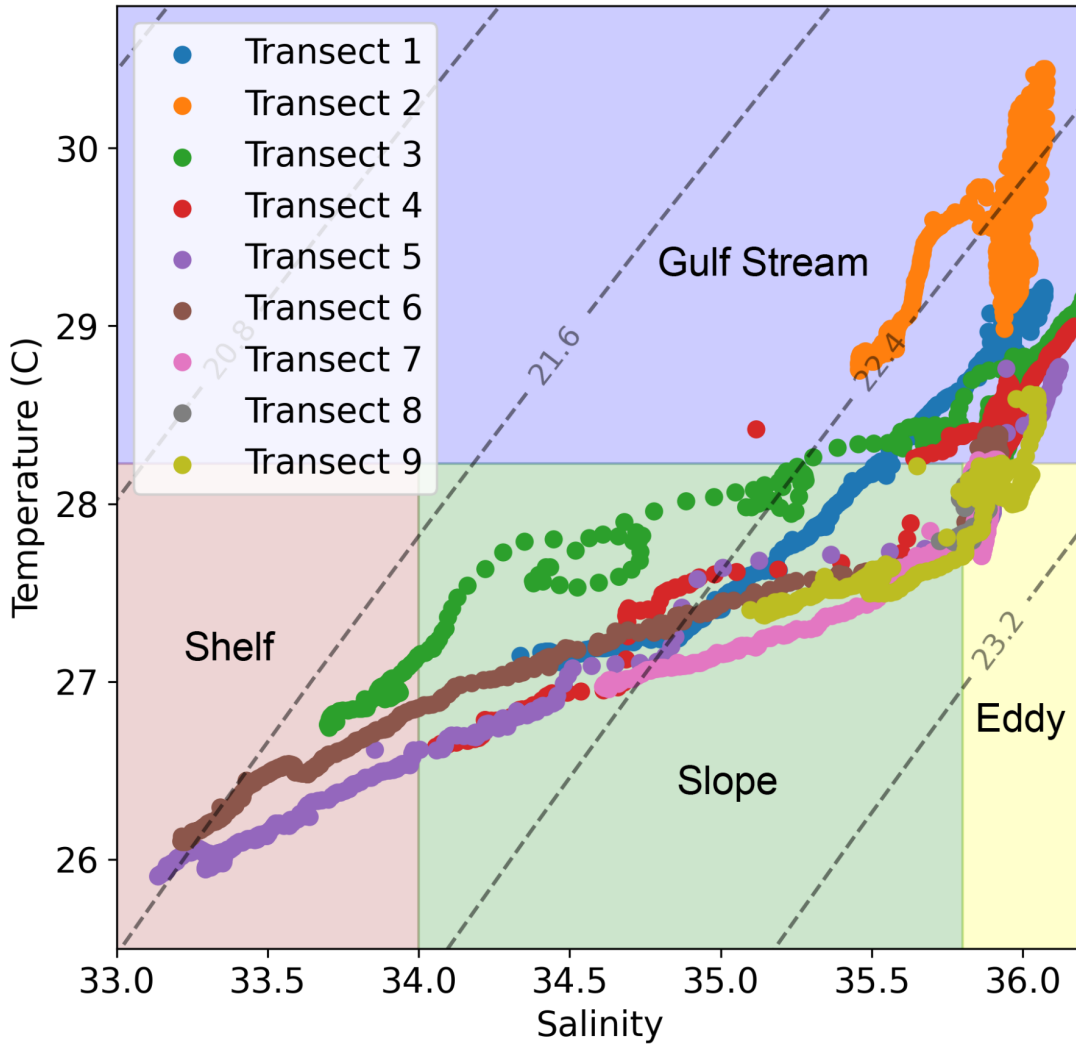
403 surprisingly γ (negatively correlated with the particle size distribution) decreases as we move
404 offshore, indicating larger particles offshore compared to inshore, in contrast to HH_G50 trends.

405 A few properties however reveal the eddy as distinct from the Gulf Stream, with depleted
406 nitrate and silicate compared to the Gulf Stream water, enhanced non-phycoerythrin containing
407 picocyanobacteria compared to all other water masses, the highest bacteria to chl-a ratio, and
408 lowest volumetric NCP (Figures 5 and 6). In the eddy c_p (460), and b_{bp} (440), and γ are marginally
409 lower compared to Gulf Stream (Figures 5 and 6).

410 Profiling data shows a MLD of ~ 10 m for shelf and slope water with eddy or Gulf Stream
411 water underlying that shallow shelf/slope water and a second thermocline around ~ 30 -50m. The
412 MLD for the eddy ranges from approximately 30-50m and Gulf Stream is the same range from
413 35-55m. Calculating MLD at the front at these scales is often problematic given the intense
414 mixing and turbulence across the front, so these exact depths should be interpreted with caution.
415 We observe a fairly consistent cold and fresh intrusion (Figure S8) moving from the shelf to the
416 Gulf Stream and converging with the Gulf Stream that could be of Arctic or northern slope origin
417 given the temperature ($<15^\circ\text{C}$) and salinity (33-33.5 PSU, comparable to shelf). While not the
418 focus of this study, this cold and relatively fresh layer has intense structuring of both chl-a
419 fluorescence and echosounder volume backscatter.

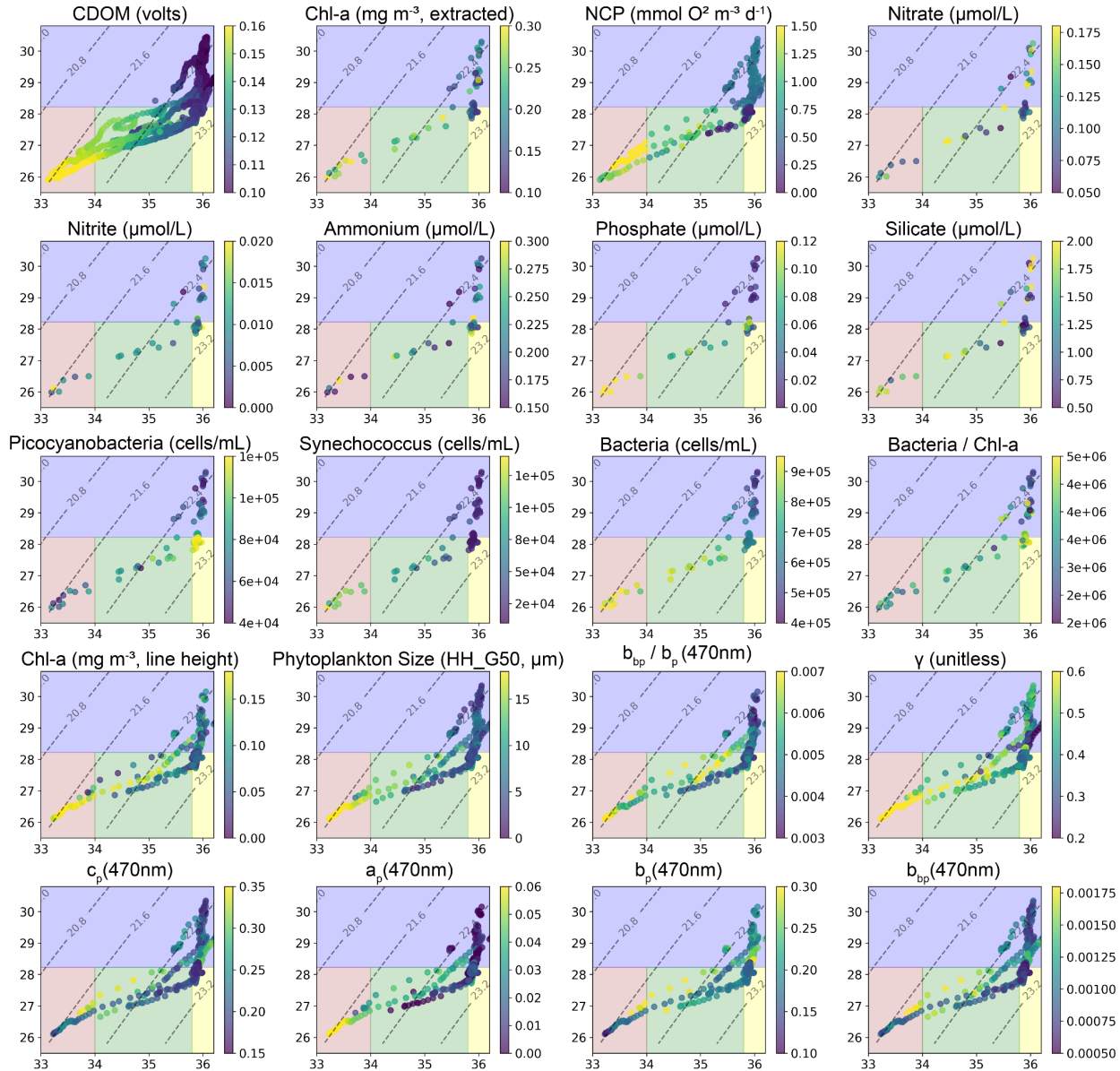
420 ADCP data supports conclusions from profiling and surface categorizations, showing
421 faster current speeds in the Gulf Stream water vs eddy water and cyclonic rotation in Transect 9
422 (T9, Figure 8). Echosounder data from the ADCP shows fairly consistent backscatter responses
423 in Gulf Stream and Eddy water and much stronger backscatter in the shallow shelf water (Figure
424 9). This acoustic backscatter data also shows a thin layer at the thermocline of the eddy that isn't
425 apparent in the Gulf Stream water (Figure 8).

426 Looking back over the satellite record indicates a monotonic decrease in chl-a at each
427 observation time step from eddy formation until our survey work (Figure 7).



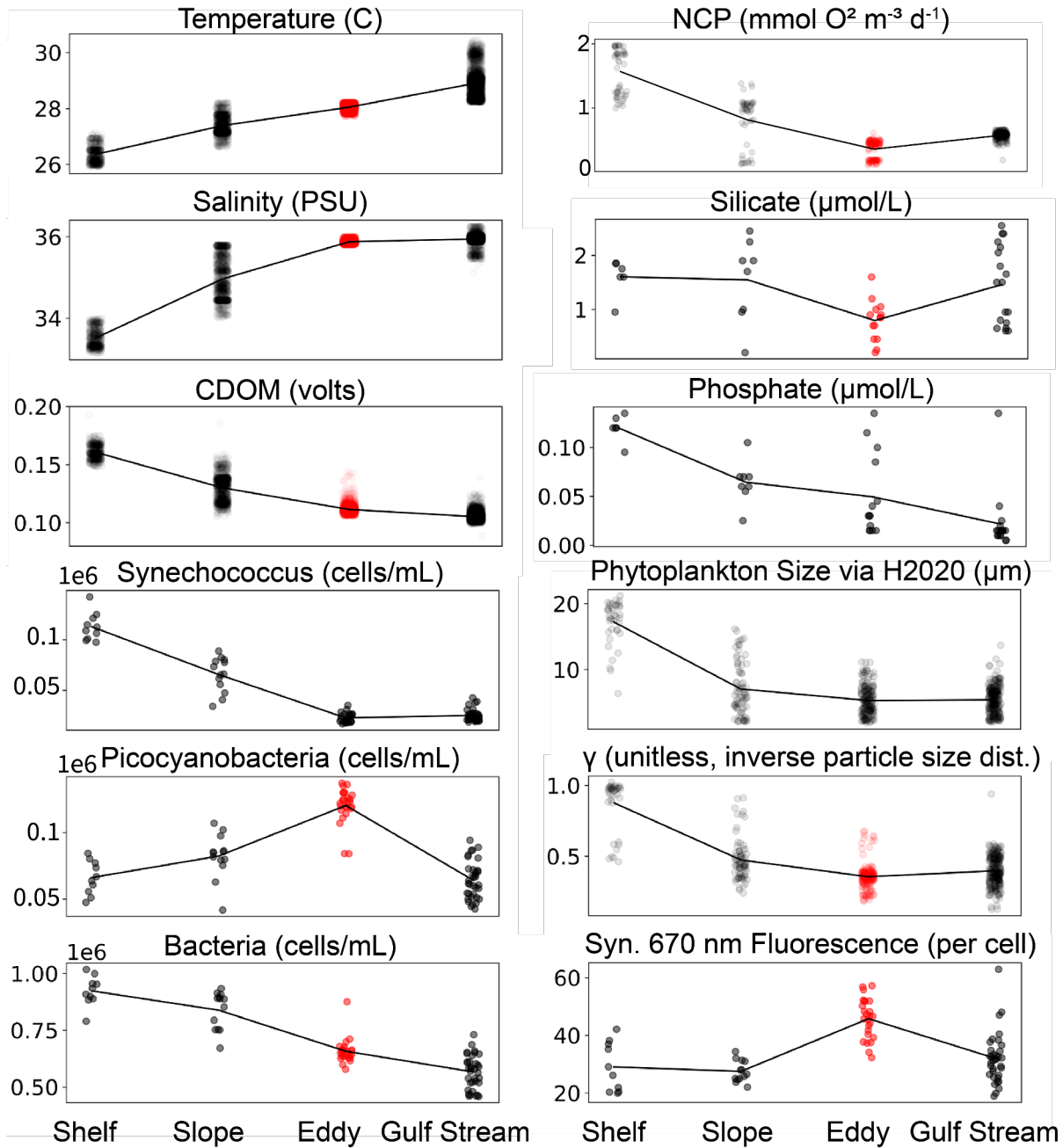
428

429 **Figure 4.** All nine transects are plotted together on a Temperature-Salinity diagram. Isopycnals
430 are shown with dashed gray lines across the plot. The reddish section with low temperature and
431 low salinity is the shelf water, green is the slope water, yellow is the eddy, and blue is the Gulf
432 Stream.
433



434

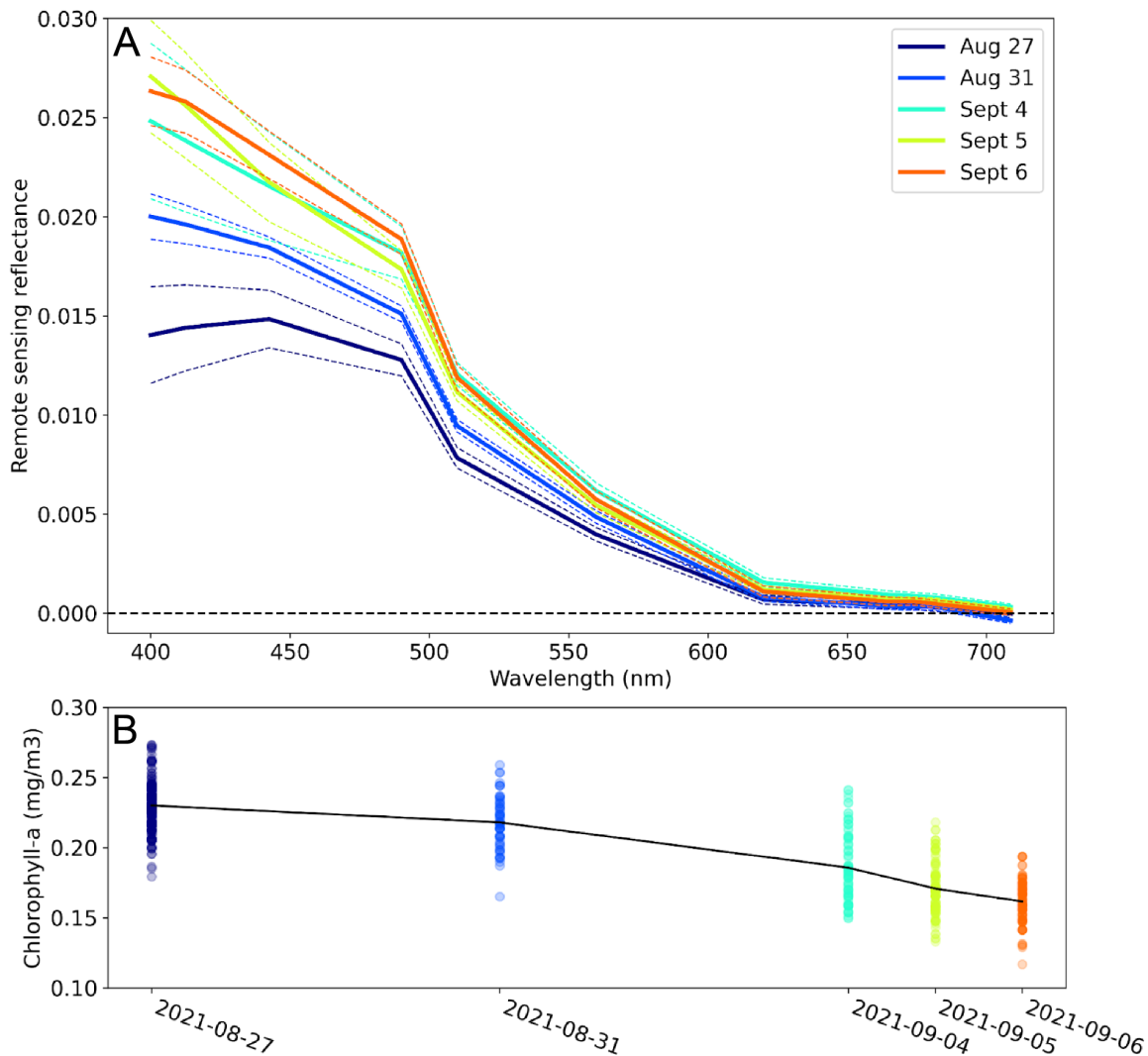
435 **Figure 5.** Measured parameters are shown on these T-S diagrams with salinity on the x-axis and
 436 temperature on the y-axis. CDOM shows the expected general trend of decreasing dissolved
 437 organic matter as you move from the shelf (colder and fresher) to the Gulf Stream (hotter and
 438 saltier). While many properties show a general increase or decrease from the Gulf Stream to the
 439 shelf - with the eddy simply near the middle or resembling the Gulf Stream properties - a few
 440 properties stand out in the eddy from either side. These are namely elevated picocyanobacteria,
 441 elevated bacteria/chla ratio, depleted silicate, and depleted nitrate.
 442



443

444 **Figure 6.** Subset of measured surface variables after classifying water masses into discrete
 445 groups (shelf, slope, eddy, and Gulf Stream) based on temperature and salinity properties. Red
 446 color in the eddy samples indicates it is statistically different from all other water masses
 447 (Welch's T-test with a p value < 0.05). Some variables are simply a continuum through these
 448 water types, monotonically decreasing as T or S increases (e.g. CDOM, bacteria, PO_4) and some
 449 properties are notably different in the eddy and could not be a simple product of mixing (e.g.
 450 picocyanobacteria, NCP, fluorescence per cell). A few variables including NO_2 , NH_4 , and NO_3
 451 are not statistically different between any water mass (e.g. $\text{NO}_3 \sim 0.1 \mu\text{mol/L}$ in all water masses).

452 Not shown here, but fluorescence per cell is nearly identical for non-phycoerythrin containing
453 picocyanobacteria.



454

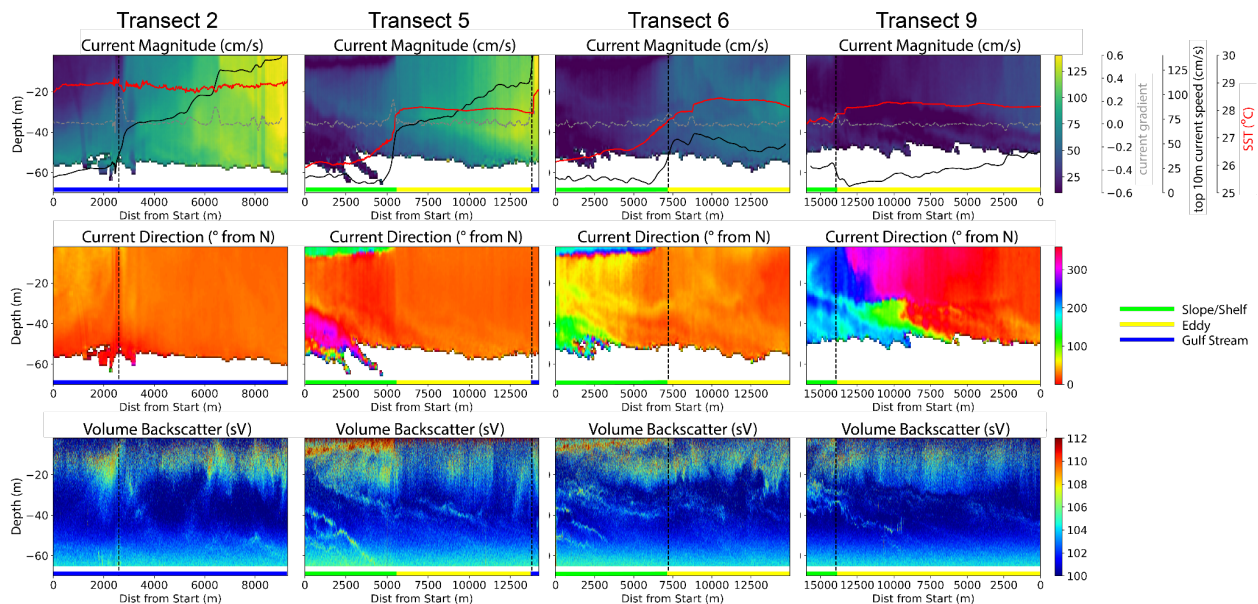
455 **Figure 7.** A. Shows median R_{rs} spectra of the eddy from the Sentinel-3 OLCI sensor over the
456 lifetime of the feature. This shows an increase in the blue wavelengths over time from the
457 formation of the eddy up until the last day it was coherent and not cloudy. Dashed lines show
458 standard deviation of spectra within the eddy. Black dashed line demarcates and R_{rs} value of 0.
459 B shows chl-a concentration (calculated via the Hu et al 2012 ocean color index) decreasing
460 monotonically throughout the observational period, the colors represent the same dates as in the
461 top panel and the black line connects the means of each time step. All satellite data used in this
462 figure shown in Figure S1.

463

464 The VMP data reveals the physical structure across all transects, with a general trend of
465 fresher and less dense shelf/slope water sitting on top of the eddy/Gulf Stream water in a thin
466 layer 5-20m and under this water is eddy or Gulf Stream water (Figure S8). Then where the

467 shelf/slope water ends at the surface the eddy/Gulf Stream water reaches the surface. The peak in
468 chl-a fluorescence from VMP data is typically around 30-50m, just below the thermocline.

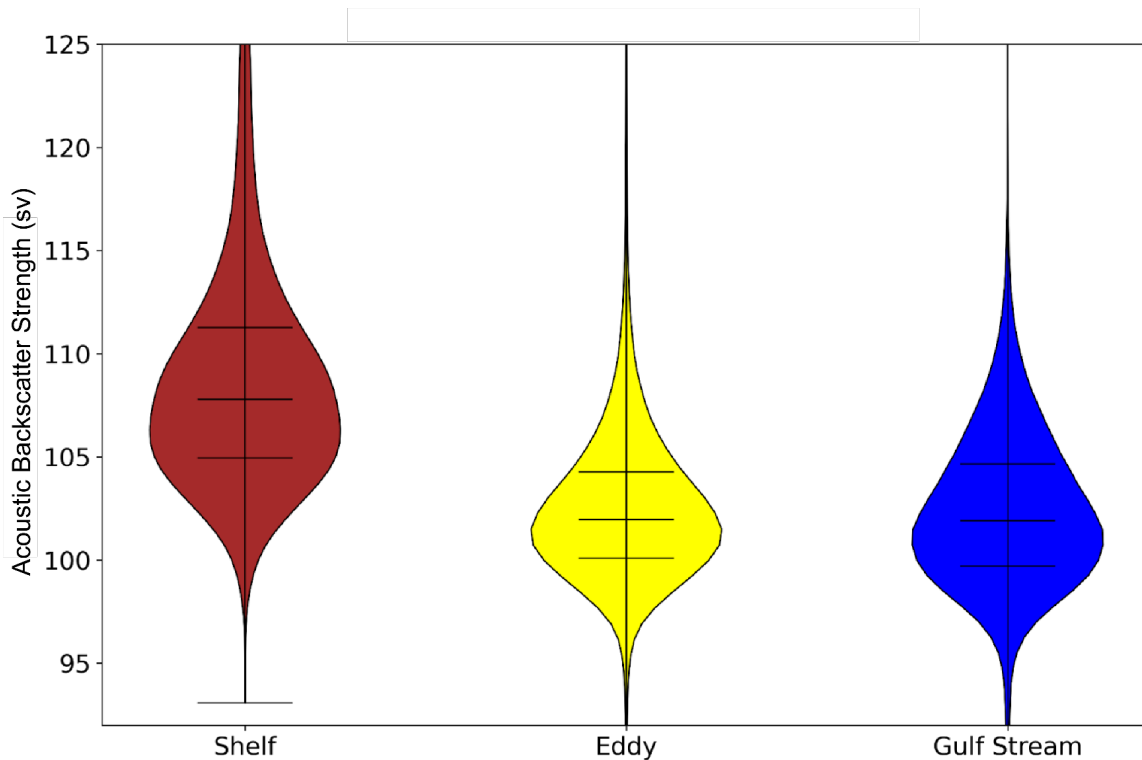
469 On the last transect of the cruise, T9, the ADCP indicates we crossed the entirety of the
470 eddy near the middle of the feature and we see strong evidence for continued rotation (Figures 8
471 and S7), though at relatively low speed ($10\text{-}40\text{ cm s}^{-1}$) compared to the Gulf Stream transects (T2,
472 150 cm s^{-1}). The ADCP also shows clear structuring of acoustic backscatter (representative of
473 zooplankton and small fish). The highest values of acoustic backscatter are in the shelf water.
474 Within the Gulf Stream and eddy water we observe high backscatter from the surface down to
475 $\sim 35\text{ m}$ (effectively the mixed layer) and then comparatively low backscatter from ~ 35 to $\sim 60\text{ m}$.
476 From 60m and deeper the data is overwhelmed by noise. As these different water masses are
477 layered physically, so are the backscatter responses. For example in Transect 6 (T6), around
478 4000 m into the transect laterally, there is highly scattering shelf water from 0-8 m, then eddy
479 water with backscatter that eventually decreases further around 30 m, followed by 3-4 thin
480 backscattering layers of 1-3 m, first at the thermocline where the eddy ends and then above and
481 below the cold water intrusion.
482



483

484 **Figure 8.** Current magnitude and direction from the ship-based ADCP are shown in the top two
485 rows and the third row shows volume backscatter from the echosounder on the ADCP. The
486 vertical dashed black line is the front as defined by the peak gradient in current, the red line is
487 sea surface temperature as measured by the ADCP, the black line is current speed, and the grey
488 line is the current gradient. Current magnitude (top panel) shows clear delineations between shelf
489 water and the eddy and the eddy and the Gulf Stream. The acoustic backscatter data (bottom
490 panel) shows the most intense backscatter in the shelf water with some possible structuring from

491 the eddy and strong thin layers from the cold water intrusion below the eddy. Note T2 data is
492 only from half of the transect due to an instrument error.



493

494 **Figure 9.** Acoustic backscatter strength across water masses from the ADCP. This is the
495 distribution of acoustic backscatter in the mixed layer for the shelf (down to 10m), eddy, and
496 Gulf Stream water (both averaged down to 40m). Means are respectively 108.97, 102.56, and
497 102.34 for the Shelf, eddy, and Gulf Stream water. ADCP measurements were not collected in
498 the slope water and thus are not represented here.

499 4 Discussion

500 Given the frequency of frontal eddies traveling along the Gulf Stream past Cape Hatteras,
501 it was our goal to understand their state after passing Cape Hatteras and the possible
502 biogeochemical impacts in the MAB. Using this information, we assess if they could help
503 explain the productivity of “the Point” of Gulf Stream separation from the continental shelf and
504 broadly how they may be impacting the MAB.

505 4.1 Eddy history

506 The satellite record (Figures 7 and S1) indicates a formation and evolution of the
507 observed frontal eddy in line with observations from previous studies and recent modeling
508 (Glenn & Ebbesmeyer, 1994b; Gula et al., 2016; T. N. Lee et al., 1991) and suggests that this
509 eddy is a typical example of a frontal eddy in this region. The eddy formed off the Charleston
510 Bump (Figure 1) driving a chl-a and SST anomaly within a Gulf Stream meander. The satellite
511 data does not show a time-evolving surface bloom compared to the initial shelf waters, but the

512 eddy does initially have higher surface chl-a than the Gulf Stream water. Over the course of two
513 weeks there is a gradual decrease in chl-a either from die off or mixing with Gulf Stream water.
514 This lack of a satellite-visible increase in chl-a when compared to the initial shelf conditions
515 could be due to enhancement of growth occurring at a depth below that detectable by satellite,
516 from a concomitant increase of grazers, or limited upwelling. We suggest it is a combination of
517 enhancement at depth and then grazers based on previous work on frontal eddies in the SAB and
518 across the globe (Glenn & Ebbesmeyer, 1994a; Gula et al., 2016; Kasai et al., 2002; Yoder et al.,
519 1981). The satellite record shows the eddy had been coherent for two weeks at the time of our in-
520 situ observations.

521 4.2 Physical status during cruise

522 During our cruise the eddy was still mostly coherent with consistent physical properties
523 across the feature and continued cyclonic rotation, which, while weak, would likely be driving a
524 negative SSH anomaly and upwelling within the eddy, possibly still enhancing productivity.
525 However, higher resolution and deeper sampling within the water column would be needed to
526 reveal the eddy's core and any stimulation of primary producer biomass.

527 On T6 we observe what is likely the remains of the frontal eddy's warm streamer that has
528 been pulled into the body of the eddy (Figure S2 for a detailed description of each transect along
529 with S and T). It is apparent from the surface to ~30m depth where temperature and salinity are
530 higher than the rest of the eddy and cell counts from flow cytometry are closer to the Gulf
531 Stream. Salinity and temperature in this warm streamer are intermediate between Gulf Stream
532 and eddy, likely representative of the intense mixing that occurs in frontal eddies (Gula et al.,
533 2016), especially past Cape Hatteras where they begin to dissipate.

534 4.3 Ecological observations

535 In spite of predicted upwelling at depth, in general the eddy has more oligotrophic
536 conditions compared to the other water masses, with lower silicate and NO_3 in the eddy
537 compared to Gulf Stream and slope waters and enhanced non-phycoerythrin containing
538 picocyanobacteria (a group which contains *Prochlorococcus*) compared to other water masses
539 (Figure 6). While cyclonic eddy dissipation will relax the isopycnal uplift, causing downwelling
540 (see Figure 5 in McGillicuddy, 2016), it is unclear exactly how this process works within frontal
541 eddies and if the timeline matches for this to help explain the more oligotrophic conditions.
542 Combined with the nutrient data which reveals lower silicate and NO_3 in the eddy compared to
543 Gulf Stream and slope waters, this suggests a shift to a microbial loop dominated system. The
544 highest bacteria to chl-a ratio occurs within the eddy, suggestive of post-bloom conditions
545 (Buchan et al., 2014). NCP is another variable in support of post-bloom conditions with the
546 lowest volumetric NCP being measured in the eddy, slightly lower than the Gulf Stream
547 conditions and substantially lower nearer the core of the eddy on the final study day (Figure 5).

548 A companion study (Gronniger et al., 2023), focused on the eddy microbiome, was
549 undertaken on the same flow-through surface samples and similarly reveals differences in
550 microbial community composition between water masses. This companion study found that the
551 eddy harbored higher abundance of *Prochlorococcus* and lower abundances of *Synechococcus*
552 and *Pelagibacteraceae*. However, despite differences between the Gulf Stream and eddy
553 microbiomes, including higher abundances of *Prochlorococcus* in the eddy and higher
554 abundances of the nitrogen-fixer *Trichodesmium* in the Gulf Stream (see also Figure 6), the eddy

555 is most similar to the Gulf Stream relative to the other water masses, suggesting that assembly of
556 the eddy microbiome is primarily determined by environmental filtering in these warm, low
557 nutrient waters. Gronniger et al (2023) clustered the microbiome data and compared this to the
558 physical delineations which showed that the discrete physical classes used here do not fully
559 reflect microbiome clusters, likely due to the intense submesoscale dynamics in this region.

560 Fluorescence per cell via flow cytometry is highest in the eddy and in frontal regions
561 (Figure 6). This was not our expectation considering higher fluorescence per cell can be
562 indicative of either more nutrients or more pigments per cell. We thus would expect the slightly
563 lower nutrient conditions in the eddy to result in lower fluorescence per cell. Because higher
564 fluorescence per cell can also indicate cells physiologically acclimatized to lower light levels,
565 this may indicate mixing from depth in these regions or higher nutrient uptake rates, not reflected
566 in free nutrient concentrations (Figure 6).

567 Acoustic backscatter shows substantial structure in all water masses (Figure 8). As
568 expected, the shelf water, which had the highest chl-a values, has the highest acoustic
569 backscatter. The Gulf Stream and eddy water are not statistically different with respect to
570 backscatter (Figure 9), though in all eddy transects there is a clear thin layer of enhancement in
571 backscatter around the thermocline of the eddy that does not appear in the Gulf Stream water
572 (Figure 8). Given the limited number of samples, it is possible this difference is related to other
573 factors and not the dynamics of the eddy itself. The cold water intrusion also appears to drive
574 thin layers in acoustic backscatter above and below the feature. Interestingly, the peak in chl-a
575 fluorescence from the VMP data is sometimes shifted down by ~15m from the acoustic
576 backscatter peak. This could be due to grazing decreasing biomass and thus fluorescence, non-
577 photochemical quenching of fluorescence in the better-lit upper layer, the relatively high
578 1000kHz sampling frequency not picking up on the grazers consuming the phytoplankton, or
579 actual partitioning in habitat. While some combination of these various factors is the most likely
580 explanation, this is nonetheless a surprising finding. It is unlikely quenching is drastically
581 different at 35m vs 45m and could suggest that in this region standing phytoplankton biomass
582 (here proxied by chl-a) is not a good representation of productivity.

583 4.4 Particle Size Surprises

584 One interesting note from this work is the divergence of γ (proxy for mean particle size)
585 from typical patterns. γ , which is sensitive to particles in the size range from approximately 3-30
586 μm (Emmanuel Boss et al., 2001), generally corresponds to chl-a concentration, based on the
587 commonly found relationship that higher chl-a corresponds to larger phytoplankton. Thus, we
588 would expect a decrease in mean particle size as we move from coastal water (high chl-a and
589 larger particles) to oligotrophic water (low chl-a and smaller particles) (Emmanuel Boss et al.,
590 2013; Buonassissi & Dierssen, 2010). In this study, we instead see an increase in particle size
591 and a decrease in chl-a as we move from shelf water further offshore into the eddy and Gulf
592 Stream (Figures 5 and 6).

593 In general, most particles in the open ocean are phytoplankton or detritus. The observed
594 increase in the mean particle size offshore is unlikely to be indicative of phytoplankton based on
595 HH_G50 which shows decreases in phytoplankton size offshore - following expectations of a
596 positive relationship between chl-a and phytoplankton size. The particles driving γ are therefore
597 unlikely to be live phytoplankton. The backscattering ratio decreases marginally as we move
598 offshore suggesting the particles influencing γ are relatively more organic, just not chl-a

599 containing. Another relevant piece of evidence, b_p is not only spectrally flatter in the Gulf Stream
600 (driving c_p to be flatter and lower γ), but actually higher overall, indicating higher particle
601 concentrations.

602 So more particles, larger average particle sizes, and particles that are similarly or
603 relatively more organic than those inshore. This leads us to the conclusion that it is either due to
604 an enhancement of small heterotrophs or possibly detritus and non-algal particles within the eddy
605 and Gulf Stream waters. This could be suggestive of grazer enhancement in the eddy, though
606 again this is not specific to the eddy. It could also be due to an accumulation of buoyant particles
607 near the front.

608 The relative consistency of γ and HH_G50 between eddy and Gulf Stream waters
609 suggests whatever process is influencing this divergence from expectations is not an eddy
610 specific phenomenon, or if it is, that the resultant particulate impact is mixed into Gulf Stream
611 waters and is possibly persistent between eddies.

612 4.5 Impact of frontal eddies on grazers

613 While relevant studies investigating consumer response to frontal eddies are rare,
614 previous work shows that copepods and doliolids increase substantially in response to
615 phytoplankton enhancement in frontal eddies. In this case these zooplankton exhibited minimal
616 vertical migration, with maxima near the thermocline, suggesting they would likely be entrained
617 in the frontal eddy and move with it north of Cape Hatteras (Paffenhöfer et al., 1987). The
618 timeline of this increase in zooplankton is variable across taxa, but in this work, the authors
619 found zooplankton increased dramatically from five days to two weeks after peak chl-a
620 concentration, and peak chl-a concentration was approximately a week after eddy formation.
621 Similar work has shown that copepods, which are slower to respond, may persist for a few
622 weeks, and doliolids which respond within days, were also found to decrease faster, persisting
623 for 7-9 days (Deibel, 1985). This work was done on the southern half of the SAB (with eddy
624 generation around Florida and dissipation just upstream of the Charleston Gyre) and may have
625 different characteristics than the northern section of our study, but if we assume similar
626 responses, zooplankton abundance should peak right when the eddy is passing Cape Hatteras.

627 Our acoustic data does not support an enhancement of zooplankton and small fish
628 biomass in the eddy compared to Gulf Stream water at the time of our measurements (Figure 9).
629 The variability of some transects adds substantial uncertainty to these comparisons and we don't
630 have a "pure" Gulf Stream endmember for comparison. Modeling shows substantial diapycnal
631 mixing between these eddies and the Gulf Stream (Gula et al., 2016), possibly contributing to the
632 lack of clear distinction in acoustic backscattering between these water masses. We do see
633 structuring of acoustic backscatter (i.e. zooplankton and fish) with a clear partitioning at the
634 thermocline of the eddy and an increase just below it which is not observed in the Gulf Stream
635 data. This could be an indicator of upwelling and higher growth. Adding to the complexity we
636 observe a large vertical migration via acoustic backscatter into the shelf and eddy water from
637 around 250 m depth. Considering our eddy has spent two nights off the shelf there is a possibility
638 a large amount of the potential grazer biomass enhancement has already been consumed by fish
639 in this migrating layer. To fully parse this out would require a Lagrangian observation approach
640 over the full lifetime of the eddy.

641 In much of the previous work on frontal eddies the assumption was that these eddies
642 decayed onto the outer shelf of the SAB, and an ongoing question was that if there is such a
643 substantial input of nutrients due to upwelling why is the outer shelf of the northern SAB not
644 more productive in higher trophic levels? We suggest based on our work and previous studies
645 that a large amount of this new production could be moving into grazer biomass, and while some
646 of this may occur on the outer shelf edge in the SAB, these features are still typically being
647 carried by the Gulf Stream into the MAB where they could contribute to the high productivity of
648 “the Point”. Even where there are subsurface intrusions far up onto the shelf of the SAB due to
649 frontal eddy upwelling this water is quickly entrained into the Gulf Stream’s northward flow, and
650 while some of this may stay on the SAB shelf long enough for the grazers to die off or be
651 consumed themselves, most of it is north of Cape Hatteras within 1-2 weeks, shown both by our
652 work and previous studies (Glenn & Ebbesmeyer, 1994a). This is a match in time for grazers to
653 have bloomed following the initial phytoplankton bloom and occurs frequently enough to sustain
654 elevated levels of secondary consumers. Previous work that did consider the entrainment of
655 carbon into the Gulf Stream from these processes framed it as a generic export process rather
656 than explicitly a potential enhancement of zooplankton being delivered directly into the mouths
657 of hungry fish in the MAB e.g. (T. N. Lee et al., 1991). In this sense the northern SAB could be
658 thought of as the breadbasket of the southern MAB with frontal eddies providing the fertilizer.

659 4.6 A refined conceptual model

660 Using insights from this work we both place our study into the context of the initial
661 conceptual model (Figure 3) and refine that model based on our new understanding.

662 We begin with the meander at the Charleston Bump which drives the Gulf Stream further
663 offshore. Due to this injection of vorticity the Charleston Gyre exists, and periodically (~3-7
664 days) drives the creation of a frontal eddy and a warm streamer of Gulf Stream water which
665 encloses this newly formed frontal eddy, partitioning it from the shelf water. We have no in-situ
666 data during this period, but previous work all supports upwelling due to the cyclonic rotation and
667 isopycnal uplift as well enhancement (compared to Gulf Stream water) from trapping during
668 eddy formation (Glenn & Ebbesmeyer, 1994b; T. N. Lee et al., 1991; Yoder et al., 1981). This
669 combination of productive shelf water and upwelling creates a chl-a anomaly well above the
670 mean. Upwelling slowly decreases as the eddy dissipates energy as it moves downstream (Gula
671 et al., 2015). The enhancement in phytoplankton growth enables an increase in grazer
672 populations, which peaks between Cape Lookout and Cape Hatteras, and sustains an enhanced
673 level of secondary consumers, possibly contributing to the high level of top predator populations
674 in this region. By the time the eddy is just north of Cape Hatteras the physics may still be driving
675 some upwelling but the phytoplankton community has switched to gleaners, possibly in a
676 microbial loop. This is where we place our study, around the secondary consumer peak and after
677 phytoplankton biomass has shifted below the baseline. After this shift to smaller cells such as
678 *Prochlorococcus*, the transfer efficiency to fish and top predators is likely to be substantially
679 lowered, adding on to the decrease in available phytoplankton (Eddy et al., 2021).

680 Our data shows the eddy from this study has depleted Si compared to Gulf Stream and
681 slope water suggesting a possible recent diatom bloom. It has the highest ratio of bacteria : chl-a
682 and lowest NCP again suggestive of post-bloom conditions. The eddy also has a higher ratio of
683 mean particle size : chl-a indicating either an enhancement of micro grazers along with the
684 picocyanobacterial or more detritus per unit chl-a. Both flow cytometry and molecular

685 sequencing show a different community composition dominated by picocyanobacteria and
686 particularly *Prochlorococcus* - again suggestive of a switch to the microbial loop. Thus we
687 hypothesize the eddy arrives at Cape Hatteras with enhanced grazer biomass due to the previous
688 phytoplankton bloom and that these grazers are consumed by the large migrating layer we
689 observed.

690 Within the SAB frontal eddies are thought to have a dominant impact on nitrogen fluxes
691 on the outer shelf (T. N. Lee et al., 1991) - with a huge impact on the ecology of the SAB outer
692 shelf. Based on our observations, frontal eddies do not appear to supply phytoplankton into the
693 MAB, but are possibly an efficient shuttle of grazers into the highly productive southern MAB
694 which is thought to have some of the highest marine mammal diversity in the world and is a
695 productive fishing ground (Byrd et al., 2014).

696 Given the complexity and dynamic nature of this region we can only hypothesize the
697 impact of frontal eddies on the overall ecosystem of the SAB and MAB (see supplemental
698 material for extended caveats). In future studies we need a Lagrangian survey approach over the
699 entire lifetime of the eddy. With acoustic backscatter and discrete net tow samples we could
700 identify the density and type of zooplankton within the eddy. In this work we focused on surface
701 samples but a large component of the frontal eddy driven enhancement may be below the
702 thermocline as it is lifted into a more favorable light environment. A fleet of autonomous assets
703 would facilitate a more synoptic view of the eddy. A survey design similar to (Zhang et al.,
704 2021) with AUVs and gliders to assess the full physical and biogeochemical status could enable
705 a test of our hypothesis. This could be an ideal exercise for high resolution modeling to examine
706 the MAB ecosystem with and without frontal eddies.

707 4.7 Broader Context

708 A similar process may be happening just upstream (south) of the Charleston Bump,
709 where the timeline matches up for the enhancement of grazers after frontal eddy enhancement
710 from Miami to Charleston and possibly complemented by a longer duration stay in the Gyre.
711 Even more generally, anywhere a western boundary current follows the continental shelf and the
712 system is nutrient limited frontal eddies may be a reliable mechanism for increasing primary
713 production and transfer efficiency to higher trophic levels.

714 5 Conclusions

715 We show in this work that frontal eddies do in fact often get advected north past Cape
716 Hatteras, can still have cyclonic rotation, and have nutrient profiles and phytoplankton
717 community compositions distinct from adjacent water masses even in dissipation. We
718 hypothesize they may be well timed to supply zooplankton to secondary consumers between
719 Cape Lookout and Cape Hatteras. Synthesizing previous literature we share a simple conceptual
720 model for the ecosystem impact of frontal eddies and place our study within that model and add
721 refinements. Given the frequency of frontal eddies moving along the Gulf Stream this may be a
722 mechanism for substantial enhancement of phytoplankton, zooplankton, and secondary
723 consumers - particularly at the highly productive separation point of the Gulf Stream jet. We
724 suggest further work on frontal eddies in the Gulf Stream and other western boundary currents to
725 see if this is a general phenomenon.

726 Acknowledgments

727 Funding support was provided by National Aeronautics and Space Administration
728 (NASA) Future Investigators in NASA Earth and Space Science and Technology (FINESST)
729 #80NSSC19K1366 (Ocean Biology and Biogeochemistry program), the Zuckerman STEM
730 Leadership Program, the American Society for Photogrammetry and Remote Sensing's Robert
731 N. Colwell Memorial Fellowship to PCG. R/V Shearwater ship time was supported by Nicholas
732 School of the Environment and Duke University Marine Lab donors through a student research
733 grant to PCG. We appreciate Emmanuel Boss for sharing instruments for the optical flow-
734 through data. Finally the authors thank the crew of the R/V Shearwater, Matt Dawson, Tina
735 Thomas, Zach Swaim, and John Wilson for making much of this data feasible and enjoyable to
736 collect.

737 Open Research

738 The code to recreate this analysis are available at <https://doi.org/10.5281/zenodo.7685135>
739 (Gray, 2023) and all data used in this study is available at
740 <https://doi.org/10.5281/zenodo.7680135> (Gray et al., 2023). All code is shared with an MIT
741 License for free reuse. We have provided multiple Jupyter Notebooks that go from raw or
742 initially processed data to the nearly complete figures shown in the paper. The python
743 environment used can be easily and exactly reproduced using the pangeo-notebook a Docker
744 image <https://github.com/pangeo-data/pangeo-docker-images/tree/master/pangeo-notebook> as
745 detailed in the Github repo.

746 References

- 747 Andres, M. (2021). Spatial and Temporal Variability of the Gulf Stream Near Cape Hatteras. *Journal of*
748 *Geophysical Research: Oceans*, 126(9), 1–21. <https://doi.org/10.1029/2021JC017579>
- 749 Arostegui, M. C., Gaube, P., Woodworth-Jefcoats, P. A., Kobayashi, D. R., & Braun, C. D. (2022). Anticyclonic
750 eddies aggregate pelagic predators in a subtropical gyre. *Nature*, 609(7927), 535–540.
751 <https://doi.org/10.1038/s41586-022-05162-6>
- 752 von Arx, W. S., Bumpus, D. F., & Richardson, W. S. (1955). On the fine-structure of the Gulf stream front. *Deep*
753 *Sea Research (1953)*, 3(1), 46–65. [https://doi.org/10.1016/0146-6313\(55\)90035-6](https://doi.org/10.1016/0146-6313(55)90035-6)
- 754 Atlas, E. L., Hager, S. W., Gordon, L. I., & Park, P. K. (1971). *A Practical Manual for Use of the Technicon*
755 *AutoAnalyzer in Seawater Nutrient Analyses Revised* (Technical Report 215, Reference 71-22).
- 756 Bane, J. M., Brooks, D. A., & Lorenson, K. R. (1981). Synoptic observations of the three-dimensional structure and
757 propagation of Gulf Stream meanders along the Carolina continental margin. *Journal of Geophysical*
758 *Research*, 86(C7), 6411. <https://doi.org/10.1029/jc086ic07p06411>
- 759 Belkin, N., Guy-Haim, T., Rubin-Blum, M., Lazar, A., Sisma-Ventura, G., Kiko, R., et al. (2022). Influence of
760 cyclonic and anticyclonic eddies on plankton in the southeastern Mediterranean Sea during late summertime.
761 *Ocean Science*, 18(3), 693–715. <https://doi.org/10.5194/os-18-693-2022>
- 762 Boss, E., Haëntjens, N., Ackleson, S., Balch, B., Chase, A., Dall'Olmo, G., et al. (2019). Inherent Optical Property
763 Measurements and Protocols: Best practices for the collection and processing of ship-based underway flow-
764 through optical data. *IOCCG Ocean Optics and Biogeochemistry Protocols for Satellite Ocean Colour Sensor*
765 *Validation*, 1–23. Retrieved from http://ioccg.org/wp-content/uploads/2017/11/inline_report_15nov2017.pdf
- 766 Boss, Emmanuel, Twardowski, M. S., & Herring, S. (2001). Shape of the particulate beam attenuation spectrum and
767 its inversion to obtain the shape of the particulate size distribution. *Applied Optics*, 40(27), 4885.
768 <https://doi.org/10.1364/ao.40.004885>
- 769 Boss, Emmanuel, Picheral, M., Leeuw, T., Chase, A., Karsenti, E., Gorsky, G., et al. (2013). The characteristics of
770 particulate absorption, scattering and attenuation coefficients in the surface ocean; Contribution of the Tara
771 Oceans expedition. *Methods in Oceanography*, 7, 52–62. <https://doi.org/10.1016/j.mio.2013.11.002>
- 772 Braun, C. D., Gaube, P., Sinclair-Taylor, T. H., Skomal, G. B., & Thorrold, S. R. (2019). Mesoscale eddies release
773 pelagic sharks from thermal constraints to foraging in the ocean twilight zone. *Proceedings of the National*

- 774 *Academy of Sciences of the United States of America*, 116(35), 17187–17192.
775 <https://doi.org/10.1073/pnas.1903067116>
- 776 Buchan, A., LeClerc, G. R., Gulvik, C. A., & González, J. M. (2014). Master recyclers: features and functions of
777 bacteria associated with phytoplankton blooms. *Nature Reviews. Microbiology*, 12(10), 686–698.
778 <https://doi.org/10.1038/nrmicro3326>
- 779 Buonassisi, C. J., & Dierssen, H. M. (2010). A regional comparison of particle size distributions and the power law
780 approximation in oceanic and estuarine surface waters. *Journal of Geophysical Research: Oceans*, 115(10).
781 <https://doi.org/10.1029/2010JC006256>
- 782 Byrd, B. L., Hohn, A. A., Lovewell, G. N., Altman, K. M., Barco, S. G., Friedlaender, A., et al. (2014). Strandings
783 as indicators of marine mammal biodiversity and human interactions off the coast of North Carolina. *Fishery*
784 *Bulletin*, 112(1), 1–23. <https://doi.org/10.7755/FB.112.1.1>
- 785 Cassar, N., Barnett, B. A., Bender, M. L., Kaiser, J., Hamme, R. C., & Tilbrook, B. (2009). Continuous high-
786 frequency dissolved O₂/Ar Measurements by Equilibrator Inlet Mass Spectrometry. *Analytical Chemistry*.
787 <https://doi.org/10.1021/ac802300u>
- 788 Chase, A., Boss, E., Zaneveld, R., Bricaud, A., Claustre, H., Ras, J., et al. (2013). Decomposition of in situ
789 particulate absorption spectra. *Methods in Oceanography*, 7, 110–124.
790 <https://doi.org/10.1016/j.mio.2014.02.002>
- 791 Chelton, D. B., Gaube, P., Schlax, M. G., Early, J. J., & Samelson, R. M. (2011). The influence of nonlinear
792 mesoscale eddies on near-surface oceanic chlorophyll. *Science*, 334(6054), 328–332.
793 <https://doi.org/10.1126/science.1208897>
- 794 Churchill, J. H., & Cornillon, P. C. (1991). Water discharged from the Gulf Stream north of Cape Hatteras. *Journal*
795 *of Geophysical Research*, 96(C12), 22227. <https://doi.org/10.1029/91jc01877>
- 796 Clayton, S., Dutkiewicz, S., Jahn, O., & Follows, M. J. (2013). Dispersal, eddies, and the diversity of marine
797 phytoplankton. *Limnology and Oceanography: Fluids and Environments*, 3(1), 182–197.
798 <https://doi.org/10.1215/21573689-2373515>
- 799 Deibel, D. (1985). Blooms of the pelagic tunicate, *Doliolotta gegenbauri*: Are they associated with Gulf Stream
800 frontal eddies? *Journal of Marine Research*, 43(1), 211–236. <https://doi.org/10.1357/002224085788437307>
- 801 Eddy, T. D., Bernhardt, J. R., Blanchard, J. L., Cheung, W. W. L., Colléter, M., du Pontavice, H., et al. (2021).
802 Energy Flow Through Marine Ecosystems: Confronting Transfer Efficiency. *Trends in Ecology and*
803 *Evolution*, 36(1), 76–86. <https://doi.org/10.1016/j.tree.2020.09.006>
- 804 Gaube, P., McGillicuddy, D. J., Chelton, D. B., Behrenfeld, M. J., & Strutton, P. G. (2014). Regional variations in
805 the influence of mesoscale eddies on near-surface chlorophyll. *Journal of Geophysical Research: Oceans*,
806 119(12), 8195–8220. <https://doi.org/10.1002/2014JC010111>
- 807 Gaube, P., Braun, C. D., Lawson, G. L., McGillicuddy, D. J., Penna, A. della, Skomal, G. B., et al. (2018).
808 Mesoscale eddies influence the movements of mature female white sharks in the Gulf Stream and Sargasso
809 Sea. *Scientific Reports*, 8(1). <https://doi.org/10.1038/s41598-018-25565-8>
- 810 Glenn, S. M., & Ebbesmeyer, C. C. (1994a). Observations of Gulf Stream frontal eddies in the vicinity of Cape
811 Hatteras. *Journal of Geophysical Research*, 99(C3), 5047–5055. <https://doi.org/10.1029/93JC02787>
- 812 Glenn, S. M., & Ebbesmeyer, C. C. (1994b). The structure and propagation of a Gulf Stream frontal eddy along the
813 North Carolina shelf break. *Journal of Geophysical Research*, 99(C3), 5029–5046.
814 <https://doi.org/10.1029/93JC02786>
- 815 Gordon, L. I., Jennings, J. C., Ross, A. A., & Krest, J. M. (1992). *A Suggested Protocol for Continuous Flow*
816 *Automated Analysis of Seawater Nutrients (Phosphate, Nitrate, Nitrite and Silicic Acid) in the WOCE*
817 *Hydrographic Program and the Joint Global Ocean Fluxes Study*. (Group Technical Report).
- 818 Gray, P. C. (2023). Code for “The Impact of Gulf Stream Frontal Eddies on Ecology and Biogeochemistry near
819 Cape Hatteras.” *Github*. <https://doi.org/10.5281/zenodo.7685135>
- 820 Gray, P. C., Gronniger, J., Savelyev, I., Dale, J., Neibergall, A., Cassar, N., et al. (2023). Data for “The Impact of
821 Gulf Stream Frontal Eddies on Ecology and Biogeochemistry near Cape Hatteras.” *Zenodo*.
822 <https://doi.org/10.5281/zenodo.7680135>
- 823 Gronniger, J., Gray, P. C., Neibergall, A., Johnson, Z., & Hunt, D. E. (2023). A Gulf Stream cold-core eddy harbors
824 a distinct microbiome compared to environmentally-similar adjacent waters. *BioRxiv*.
825 <https://doi.org/10.1101/2023.02.23.529726>
- 826 Gula, J., Molemaker, M. J., & McWilliams, J. C. (2015). Gulf stream dynamics along the southeastern U.S.
827 seaboard. *Journal of Physical Oceanography*, 45(3), 690–715. <https://doi.org/10.1175/JPO-D-14-0154.1>

- 828 Gula, J., Molemaker, M. J., & McWilliams, J. C. (2016). Submesoscale dynamics of a Gulf Stream frontal eddy in
829 the South Atlantic Bight. *Journal of Physical Oceanography*, 46(1), 305–325. [https://doi.org/10.1175/JPO-D-](https://doi.org/10.1175/JPO-D-14-0258.1)
830 14-0258.1
- 831 Haëntjens, N., & Boss, E. (2020). Inlinino: A Modular Software Data Logger for Oceanography. *Oceanography*,
832 33(1), 80–84. <https://doi.org/10.5670/oceanog.2020.112>
- 833 Hager, S. W., Atlas, E. L., Gordon, L. I., Mantyla, A. W., & Park, P. K. (1972). A COMPARISON AT SEA OF
834 MANUAL AND AUTOANALYZER ANALYSES OF PHOSPHATE, NITRATE, AND SILICATE I.
835 *Limnology and Oceanography*, 17(6), 931–937. <https://doi.org/10.4319/lo.1972.17.6.0931>
- 836 Haney, J. (1986). Seabird segregation at Gulf Stream frontal eddies. *Marine Ecology Progress Series*.
837 <https://doi.org/10.3354/meps028279>
- 838 Houskeeper, H. F., Draper, D., Kudela, R. M., & Boss, E. (2020). Chlorophyll absorption and phytoplankton size
839 information inferred from hyperspectral particulate beam attenuation. *Applied Optics*, 59(22), 6765.
840 <https://doi.org/10.1364/ao.396832>
- 841 Hsu, A. C., Boustany, A. M., Roberts, J. J., Chang, J. H., & Halpin, P. N. (2015). Tuna and swordfish catch in the
842 U.S. northwest Atlantic longline fishery in relation to mesoscale eddies. *Fisheries Oceanography*, 24(6), 508–
843 520. <https://doi.org/10.1111/fog.12125>
- 844 Johnson, Z. I., Shyam, R., Ritchie, A. E., Mioni, C., Lance, V. P., Murray, J. W., & Zinser, E. R. (2010). The effect
845 of iron-and light-limitation on phytoplankton communities of deep chlorophyll maxima of the western Pacific
846 Ocean. *Journal of Marine Research*, 68(2), 283–308. <https://doi.org/10.1357/002224010793721433>
- 847 Kasai, A., Kimura, S., Nakata, H., & Okazaki, Y. (2002). Entrainment of coastal water into a frontal eddy of the
848 Kuroshio and its biological significance. *Journal of Marine Systems*, 37(1–3), 185–198.
849 [https://doi.org/10.1016/S0924-7963\(02\)00201-4](https://doi.org/10.1016/S0924-7963(02)00201-4)
- 850 Kimura, S., Kasai, A., Nakata, H., Sugimoto, T., Simpson, J. H., & Cheok, J. V. S. (1997). Biological productivity
851 of meso-scale eddies caused by frontal disturbances in the Kuroshio. *ICES Journal of Marine Science*, 54(2),
852 179–192. <https://doi.org/10.1006/jmsc.1996.0209>
- 853 Landry, M. R., Brown, S. L., Rii, Y. M., Selph, K. E., Bidigare, R. R., Yang, E. J., & Simmons, M. P. (2008).
854 Depth-stratified phytoplankton dynamics in Cyclone Opal, a subtropical mesoscale eddy. *Deep-Sea Research*
855 *Part II: Topical Studies in Oceanography*, 55(10–13), 1348–1359. <https://doi.org/10.1016/j.dsr2.2008.02.001>
- 856 Lee, T. N., Yoder, J. A., & Atkinson, L. P. (1991). Gulf Stream frontal eddy influence on productivity of the
857 southeast US Continental Shelf. *Journal of Geophysical Research*, 96(C12), 191–205.
858 <https://doi.org/10.1029/91jc02450>
- 859 Lee, Thomas N. (1975). Florida current spin-off eddies. *Deep Sea Research and Oceanographic Abstracts*, 22(11),
860 753–765. [https://doi.org/10.1016/0011-7471\(75\)90080-7](https://doi.org/10.1016/0011-7471(75)90080-7)
- 861 Lee, Thomas N., Atkinson, L. P., & Legeckis, R. (1981). Observations of a Gulf Stream frontal eddy on the Georgia
862 continental shelf, April 1977. *Deep Sea Research Part A, Oceanographic Research Papers*, 28(4), 347–378.
863 [https://doi.org/10.1016/0198-0149\(81\)90004-2](https://doi.org/10.1016/0198-0149(81)90004-2)
- 864 Lévy, M. (2008). The Modulation of Biological Production by Oceanic Mesoscale Turbulence. In *Transport and*
865 *Mixing in Geophysical Flows* (pp. 219–261). Berlin, Heidelberg: Springer Berlin Heidelberg.
866 https://doi.org/10.1007/978-3-540-75215-8_9
- 867 Lévy, M., Jahn, O., Dutkiewicz, S., Follows, M. J., & D’Ovidio, F. (2015). The dynamical landscape of marine
868 phytoplankton diversity. *Journal of the Royal Society Interface*, 12(111).
869 <https://doi.org/10.1098/rsif.2015.0481>
- 870 Lévy, M., Franks, P. J. S., & Smith, K. S. (2018). The role of submesoscale currents in structuring marine
871 ecosystems. *Nature Communications*. <https://doi.org/10.1038/s41467-018-07059-3>
- 872 Mahadevan, A. (2016). The Impact of Submesoscale Physics on Primary Productivity of Plankton. *Annual Review of*
873 *Marine Science*, 8(1), 161–184. <https://doi.org/10.1146/annurev-marine-010814-015912>
- 874 Marie, D., Partensky, F., Jacquet, S., & Vaultot, D. (1997). Enumeration and Cell Cycle Analysis of Natural
875 Populations of Marine Picoplankton by Flow Cytometry Using the Nucleic Acid Stain SYBR Green I. *Applied*
876 *and Environmental Microbiology*, 63(1), 186–193. <https://doi.org/10.1128/aem.63.1.186-193.1997>
- 877 Maul, G. A., Norris, D. R., & Johnson, W. R. (1974). Satellite photography of eddies in the Gulf Loop Current.
878 *Geophysical Research Letters*, 1(6), 256–258. <https://doi.org/10.1029/GL001i006p00256>
- 879 McClain, C. R., & Atkinson, L. P. (1985). A note on the Charleston Gyre. *Journal of Geophysical Research*, 90(C6),
880 11857. <https://doi.org/10.1029/JC090iC06p11857>
- 881 McGillicuddy, D. J. (2016). *Mechanisms of Physical-Biological-Biogeochemical Interaction at the Oceanic*
882 *Mesoscale*. *Annual Review of Marine Science* (Vol. 8). [https://doi.org/10.1146/annurev-marine-010814-](https://doi.org/10.1146/annurev-marine-010814-015606)
883 015606

- 884 Paffenhöfer, G. A., Sherman, B. K., & Lee, T. N. (1987). Abundance, distribution and patch formation of
885 zooplankton. *Progress in Oceanography*, 19(3–4), 403–436. [https://doi.org/10.1016/0079-6611\(87\)90016-4](https://doi.org/10.1016/0079-6611(87)90016-4)
- 886 Pelegri, J. L., & Csanady, G. T. (1991). Nutrient transport and mixing in the gulf stream. *Journal of Geophysical*
887 *Research: Oceans*, 96(C2), 2577–2583. <https://doi.org/10.1029/90JC02535>
- 888 Pillsbury, J. (1890). The Gulf Stream: Methods of the Investigation and Results of the Research. *Annual Report of*
889 *the Coast and Geodetic Survey, Appendix N*.
- 890 Reuer, M. K., Barnett, B. A., Bender, M. L., Falkowski, P. G., & Hendricks, M. B. (2007). New estimates of
891 Southern Ocean biological production rates from O₂/Ar ratios and the triple isotope composition of O₂. *Deep-*
892 *Sea Research Part I: Oceanographic Research Papers*, 54(6), 951–974.
893 <https://doi.org/10.1016/j.dsr.2007.02.007>
- 894 Ribbe, J., Toasperm, L., Wolff, J. O., & Ismail, M. F. A. (2018). Frontal eddies along a western boundary current.
895 *Continental Shelf Research*, 165, 51–59. <https://doi.org/10.1016/j.csr.2018.06.007>
- 896 Rudnick, D. L., Gopalakrishnan, G., & Cornuelle, B. D. (2015). Cyclonic eddies in the Gulf of Mexico:
897 Observations by underwater gliders and simulations by numerical model. *Journal of Physical Oceanography*,
898 45(1), 313–326. <https://doi.org/10.1175/JPO-D-14-0138.1>
- 899 Sathyendranath, S., Brewin, R., Brockmann, C., Brotas, V., Calton, B., Chuprin, A., et al. (2019). An Ocean-Colour
900 Time Series for Use in Climate Studies: The Experience of the Ocean-Colour Climate Change Initiative (OC-
901 CCI). *Sensors*, 19(19), 4285. <https://doi.org/10.3390/s19194285>
- 902 Schaeffer, A., Gramoulle, A., Roughan, M., & Mantovanelli, A. (2017). Characterizing frontal eddies along the East
903 Australian Current from HF radar observations. *Journal of Geophysical Research: Oceans*, 122(5), 3964–
904 3980. <https://doi.org/10.1002/2016JC012171>
- 905 Seim, H., Savidge, D., Andres, M., Bane, J., Edwards, C., Gawarkiewicz, G., et al. (2022). Overview of the
906 Processes Driving Exchange at Cape Hatteras Program. *Oceanography*.
907 <https://doi.org/10.5670/oceanog.2022.205>
- 908 Slade, W. H., Boss, E., Dall'olmo, G., Langner, M. R., Loftin, J., Behrenfeld, M. J., et al. (2010). Underway and
909 moored methods for improving accuracy in measurement of spectral particulate absorption and attenuation.
910 *Journal of Atmospheric and Oceanic Technology*, 27(10), 1733–1746.
911 <https://doi.org/10.1175/2010JTECHO755.1>
- 912 Teeter, L., Hamme, R. C., Ianson, D., & Bianucci, L. (2018). Accurate Estimation of Net Community Production
913 From O₂/Ar Measurements. *Global Biogeochemical Cycles*, 32(8), 1163–1181.
914 <https://doi.org/10.1029/2017GB005874>
- 915 Twardowski, M. S., Boss, E., Macdonald, J. B., Pegau, W. S., Barnard, A. H., & Zaneveld, J. R. v. (2001). A model
916 for estimating bulk refractive index from the optical backscattering ratio and the implications for
917 understanding particle composition in case I and case II waters. *Journal of Geophysical Research: Oceans*,
918 106(C7), 14129–14142. <https://doi.org/10.1029/2000jc000404>
- 919 Wanninkhof, R. (2014). Relationship between wind speed and gas exchange over the ocean revisited. *Limnology*
920 *and Oceanography: Methods*, 12(JUN), 351–362. <https://doi.org/10.4319/lom.2014.12.351>
- 921 Webster, F. (1961). The Effect of Meanders on the Kinetic Energy Balance of the Gulf Stream. *Tellus*, 13(3), 392–
922 401. <https://doi.org/10.1111/j.2153-3490.1961.tb00100.x>
- 923 Williams, R. G., & Follows, M. J. (1998). The Ekman transfer of nutrients and maintenance of new production over
924 the North Atlantic. *Deep-Sea Research Part I: Oceanographic Research Papers*, 45(2–3), 461–489.
925 [https://doi.org/10.1016/S0967-0637\(97\)00094-0](https://doi.org/10.1016/S0967-0637(97)00094-0)
- 926 Yoder, J. A., Atkinson, L. P., Lee, T. N., Kim, H. H., & McClain, C. R. (1981). Role of Gulf Stream frontal eddies
927 in forming phytoplankton patches on the outer southeastern shelf. *Limnology and Oceanography*, 26(6), 1103–
928 1110. <https://doi.org/10.4319/lo.1981.26.6.1103>
- 929 Zhang, Y., Ryan, J. P., Hobson, B. W., Kieft, B., Romano, A., Barone, B., et al. (2021). A system of coordinated
930 autonomous robots for Lagrangian studies of microbes in the oceanic deep chlorophyll maximum. *Science*
931 *Robotics*, 6(50). <https://doi.org/10.1126/scirobotics.abb9138>